agriculture

MDPI

*Article*

# A Novel Drought-Resistance Index Balancing Foxtail Millet Yield and Quality and Its Prediction Based on UAV Multimodal Data

**Jinyu Qin [1], Wenying Zhang [2,*], Jinhang Liu [3], Yongfeng Wu [3,*], Weilong Qin [2], Bianyin Wang [2], Zhaoyang Chen [2], Binhui Liu [2], Yajie Liu [2], Youqi Wang [4] and Bo Yang [1]**

[1] School of Geographical Sciences, Hunan Normal University, Changsha 410081, China
[2] Dryland Farming Institute, Hebei Academy of Agriculture and Forestry Sciences/Key Laboratory of Crop Drought Tolerance Research of Hebei Province, Hengshui 053000, China
[3] Institute of Environment and Sustainable Development in Agriculture, Chinese Academy of Agricultural Sciences, Beijing 100081, China
[4] Dayu College, Hohai University, Nanjing 210024, China
* Correspondence: wenyingzhang@haafs.ac.cn (W.Z.); wuyongfeng@caas.cn (Y.W.)

**Abstract**

Drought stress severely limits foxtail millet yield and quality, yet current drought-resistance indices are exclusively yield-oriented and ignore grain-filling quality. Our two-year (2024–2025) experiments with 24–48 varieties revealed that yield and blighted grain rate (BGR) are partially decoupled (e.g., Zhangzagu 18: yield 2307 kg/ha, BGR 0.444; Zhonggu 19: yield 1622 kg/ha, BGR 0.280). We therefore constructed the Yield–Quality Synergy Index (YQSI = DYI − BGR), which penalizes varieties with poor grain filling. The YQSI tied for first place with DYI in comprehensive screening performance and achieved the highest inter-annual stability (Spearman $\varrho$ = 0.823, Jaccard = 0.438, composite score = 1.261). Sensitivity analysis confirmed robustness of the equal-weight formula across a 4-fold range of quality-penalty weights. Six strongly drought-resistant germplasms with balanced yield and quality were identified. Using UAV multimodal data (RGB, multispectral, and thermal infrared) acquired during grain filling, a Random Forest model predicted a YQSI with overall $R^2$ = 0.819 and an F1 score of 0.933 for variety screening. Feature-importance analysis highlighted NDVI, WDRVI, and red-edge texture as key predictors. This study provides a quality-constrained drought-resistance evaluation framework and demonstrates the potential of UAV-based high-throughput phenotyping for foxtail millet breeding.

**Keywords:** foxtail millet; Yield–Quality Synergy Index (YQSI); blighted grain rate; UAV multimodal remote sensing; Random Forest; drought-resistance screening

Academic Editor: Mavromatis Theodoros

Received: 20 July 2026
Revised: 13 August 2026
Accepted: 15 August 2026
Published: 17 August 2026



## 1. Introduction

Foxtail millet (*Setaria italica* L.) is a traditional minor cereal crop with a long history of cultivation in the dryland farming regions of northern China, where it contributes to diversifying dietary patterns and optimizing cropping systems. Its outstanding tolerance to drought and low fertility makes it particularly suitable for cultivation in arid and semi-arid areas [1,2]. Under global climate change, however, drought stress is becoming more frequent and intense. Drought stress not only reduces foxtail millet yield by 10–30%, but also severely inhibits grain filling, resulting in a higher blighted grain rate and poorer quality [3,4]. Therefore, achieving synergistic improvement of both yield and quality under drought conditions has become an issue that demands attention in current breeding and production practices.

Accurate evaluation of crop drought resistance is a prerequisite for drought-resistant breeding. Since the 1980s, researchers have developed various drought-resistance indices based on yield performance. Broadly, these can be divided into three categories. One category comprises stability-oriented indices, such as the Yield Stability Index (YSI) [5] and Drought Stress Susceptibility Index (DSSI) [6], which measure the fluctuation of crop variety yield under different water regimes. A second category consists of yield-oriented indices, such as the Drought Yield Index (DYI) [7], Mean Productivity (MP) and Geometric Mean Productivity (GMP) [8,9], which directly reflect the productivity of varieties under drought or non-drought conditions. A third category comprises comprehensive indices, such as the Drought-Resistance Index (DRI) [10], Drought Stress Tolerance Index (DSTI) and Stress Tolerance Index (STI) [9,11], which attempt to balance yield level and stability. These indices have been widely applied to wheat [12,13], maize [14], common bean [15] and other crops, providing important tools for screening drought-resistant germplasm.

However, existing drought-resistance indices share a common drawback: they are overwhelmingly yield-oriented. They focus primarily on yield and neglect the profound effects of drought stress on quality traits. More critically, drought stress not only reduces the number of grains, but also inhibits the transport of assimilates for grain filling, thereby leading to poor grain plumpness [16,17]. As a core indicator of grain-filling plumpness, blighted grain rate directly reflects the efficiency of assimilate transport to grains and starch synthesis [18,19]. From a physiological perspective, more than 90% of cereal grain weight is starch. Grain filling depends on two key processes: the efficiency of transporting photosynthetic assimilates (as sucrose) from source organs to grains, and the efficiency of converting sucrose into starch for accumulation in grains [17]. Drought stress disrupts both processes. On the one hand, water deficit reduces leaf photosynthetic rate and assimilate supply; on the other hand, it inhibits the activities of key filling enzymes such as sucrose synthase and ADP-glucose pyrophosphorylase, thereby hindering starch synthesis. The final result is poor grain plumpness and an increased blighted grain rate [16,20]. Therefore, blighted grain rate not only determines milling yield and commercial grade, but also serves as a direct reflection of filling efficiency, and it has a non-linear relationship with yield [21]. Studies have shown that there are significant genetic differences in filling efficiency under drought among foxtail millet varieties [2,22], indicating that high yield does not necessarily imply good quality and drought resistance does not guarantee normal filling. However, no existing drought-resistance index incorporates quality traits such as blighted grain rate. As a result, selected drought-resistant varieties may have high yield but poor quality, while truly drought-resistant varieties with high filling efficiency and plump grains may be overlooked. Thus, including blighted grain rate in foxtail millet drought-resistance evaluation essentially introduces a filling-efficiency constraint, selecting varieties that maintain efficient assimilate transport and synthesis under drought conditions.

Nevertheless, incorporating blighted grain rate also creates new data acquisition pressure. Traditional determination of blighted grain rate relies on manual water or air separation, which is time-consuming, labour-intensive and subjective. It is difficult to obtain as quickly as yield through plot harvesting, so early-generation breeding materials generally lack quality evaluation data [18]. To overcome this bottleneck, Liu et al. [18,19] proposed an image analysis method based on grain shadow features, using multi-source illumination imaging to automatically identify blighted and plump grains, thus enabling rapid non-destructive measurement of blighted grain rate. However, this method is

https://doi.org/10.3390/agriculture16161765

mainly suitable for indoor or in vitro grain analysis, and is not yet directly applicable to the simultaneous, high-throughput calculation of blighted grain rate for many varieties (lines) in the field. Therefore, the present study adopted a dry-weight-based method for calculating blighted grain rate: after full maturity, whole panicles are dried and then weighed to obtain panicle dry weight and grain dry weight. This method directly uses the oven-drying and weighing data from the conventional trait-evaluation process, requiring no additional equipment or subjective judgment. It simultaneously obtains panicle dry weight and grain dry weight for all plots, enabling objective, batch calculation of blighted grain rate, and it seamlessly integrates with traits such as harvest index and yield.

In recent years, the rapid development of unmanned aerial vehicle (UAV) remote sensing technology has provided new technical support for the non-destructive, high-throughput acquisition of crop canopy phenotypic information at the field scale [23,24]. A review of previous studies reveals two main technical approaches for using UAV remote sensing to estimate crop drought-resistance indices. The first approach directly predicts the drought-resistance index from UAV data [11,25]. The second approach predicts crop yield under different treatments from UAV data and then calculates the drought-resistance index from the predicted yield [26]. Studies have shown that the accuracy of directly predicting drought-resistance indices is not lower than that of first predicting yield and then calculating the index. For example, Li et al. [11] directly predicted a wheat drought-resistance index using multi-modal data fusion and achieved accuracy comparable to yield prediction. Zhu et al. [25] also found that a comprehensive drought-resistance evaluation index directly constructed from UAV multi-source data could effectively distinguish different drought-resistance levels among wheat germplasms. Therefore, with the support of UAV multimodal data, the data acquisition pressure introduced by including blighted grain rate in a new foxtail millet drought-resistance index can be effectively alleviated.

Based on the above analysis, this study proposes two core scientific questions. The first is whether we can construct a novel drought-resistance index that balances yield and quality (constrained by blighted grain rate) and that outperforms traditional yield-oriented indices in screening high-quality drought-resistant varieties. The second is whether we can accurately predict this index using UAV multimodal data acquired after heading. To address these questions, we conducted a water-stress experiment over a two-year period (2024 - 2025) in Hengshui, Hebei Province, China. We propose the Yield–Quality Synergy Index (YQSI) to comprehensively characterise drought resistance in foxtail millet. Using Yugu 18 as the empirical reference variety, we systematically compared the performance of YQSI and eight existing drought-resistance indices in screening drought-resistant varieties. Based on UAV multimodal data, we constructed a YQSI prediction model using Random Forest and comprehensively evaluated its prediction accuracy.

## 2. Materials and Methods

### *2.1. Experimental Design and Plant Material*

The experiments were conducted in 2024 and 2025 at the experimental station of the Dryland Agriculture Research Institute in Hengshui, Hebei Province (115°42′ E, 37°54′ N). This region has a typical temperate continental monsoon climate, with an average annual precipitation of 497.1 mm, of which 70% falls in July and August. The average annual temperature is 12.5 °C, and the frost-free period is about 200 days. This area represents a typical dryland farming region of the North China Plain.

The plant material comprised 24 varieties in 2024, and was increased to 48 varieties in 2025 (including the original 24) (Figure 1). All varieties are conventional cultivars with a growth period of 105–125 days, covering the main genetic backgrounds of the summer millet region of North China. The experiment was conducted under a movable rainout shelter equipped with a precision drip-irrigation control system to exclude natural precipitation. Each variety was subjected to three water treatments, each with three replicates, and each replicate was a separate plot.

Before sowing, all plots were fully irrigated to ensure seedling emergence. The three water treatments for each variety were as follows. (1) Non-Watered (NW): no irrigation throughout the growing season. (2) Deficit-Watered (DW): irrigation applied only at heading, with an amount of 75 mm. (3) Well-Watered (WW): irrigation applied at heading and flowering, two irrigations in total, each of 75 mm, summing to 150 mm. Concrete water barriers (15 cm wide, 5 cm high) were placed between treatments and around individual plots to prevent lateral water seepage and ensure independent soil columns.

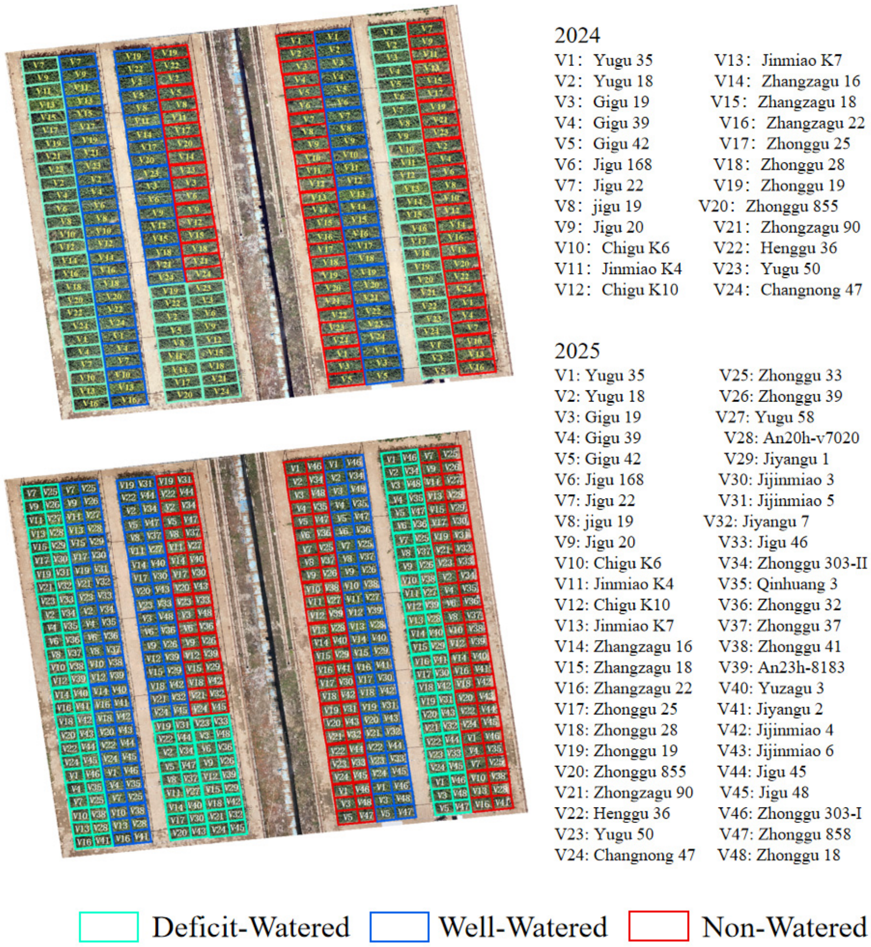


**Figure 1.** Experimental design and variety distribution in the two years.

In 2024, each plot measured 2.2 m × 1.0 m, and there were 27 × 8 = 216 plots. In 2025, the number of varieties doubled compared with the previous year. Each plot was halved in size with a 20 cm protected zone in the middle for strict water isolation. Thus, in 2025, each plot measured 1 m × 1 m, and there were 27 × 16 = 432 plots (Figure 1). Yield was determined by whole-plot harvesting, ensuring that edge effects were fully incorporated, regardless of plot dimensions. Before sowing, all plots were uniformly irrigated to about 80% of field capacity to ensure consistent emergence. Sowing dates were 14 June 2024 and 16 June 2025. Pest, disease and weed management followed local conventional practices during the growing season.

### 2.2. Data Collection and Preprocessing

#### 2.2.1. Agronomic Trait Collection and Preprocessing

Yield and trait evaluation were conducted at the full maturity stage. All plants in each plot were harvested manually. All panicles were collected, placed in mesh bags, air-dried to constant weight, and then threshed. After threshing, grains were further air-dried to about 13% moisture content, weighed, and converted to hectare yield (kg/ha).

At the same time, all plants in each plot were taken for trait evaluation. Panicles were separated from stems and leaves. Panicles were placed in kraft paper bags, oven-dried at 105 °C for 30 min and then at 80 °C to constant weight, and panicle dry weight was recorded. After manual threshing, grains were separated from glumes and rachises. Grains were oven-dried to constant weight and grain dry weight was recorded. Stems and leaves were oven-dried to constant weight, and the total dry weight of stems and leaves was recorded. These data were used to calculate blighted grain rate and harvest index.

#### 2.2.2. UAV Multimodal Data Collection and Preprocessing

UAV flights were conducted during the grain-filling stage between 11:00 and 13:00 Beijing time. A DJI Mavic 3 Multispectral (DJI M3M) UAV (M3M, DJI Technology Co., Ltd., Shenzhen, China) was used to simultaneously acquire multispectral images in four bands: green (550 ± 16 nm), red (650 ± 16 nm), red edge (730 ± 16 nm) and near-infrared (860 ± 26 nm). Simultaneously, a DJI Mavic 3 Thermal (DJI M3T) UAV (M3T, DJI Technology Co., Ltd., Shenzhen, China) was used to acquire thermal infrared images (8–14 μm, 30 Hz, 640 × 512 pixels). Flight altitude was 12 m, with ground resolutions of 0.54 cm for multispectral and 1.4 cm for thermal infrared. Heading overlap was 85% and side overlap 75%. Both UAVs were integrated with RTK modules for centimetre-level positioning. Before each flight, a 50% standard reflectance grey panel was placed in the experimental field for radiometric calibration of multispectral images, and black and white acrylic panels were placed for temperature calibration of thermal infrared images.

Radiometric calibration of multispectral images followed a two-step procedure. First, the built-in downwelling light sensor (DLS) of the M3M recorded light intensity in real time, and Pix4D Mapper software (Pix4D SA, Lausanne, Switzerland) automatically converted raw DN values to apparent reflectance. Then, absolute reflectance calibration was performed using the known reflectance (50%) of the grey panel to obtain surface reflectance in the range 0–1. Thermal infrared images were converted from raw R-JPEG to GeoTIFF temperature images using the DJI Thermal SDK, and then mosaicked into orthomosaics using Agisoft Metashape (Agisoft LLC, Petersburg, Russia). Linear correction between UAV-derived temperature values and those measured by a FLIR handheld thermal imager (using the black and white acrylic panels) was applied ($R^2 > 0.97$), to ensure temperature accuracy.

An adaptive image-segmentation algorithm [27] was used to extract pure foxtail millet canopy pixels, effectively removing soil and shadow backgrounds and ensuring that plot size differences did not affect the physical meaning of the extracted canopy reflectance. The reflectance and temperature values of all canopy pixels within each plot were averaged to obtain the spectral features and canopy temperature for that plot. Based on multispectral and thermal data, we calculated 53 spectral indices (see Appendix A) for subsequent analysis.

### 2.3. Calculation of Current Agronomic Indices and Drought-Resistance Indices

#### 2.3.1. Blighted Grain Rate

Blighted Grain Rate (BGR) is defined as the difference between panicle dry weight and grain dry weight divided by panicle dry weight. It is used to characterise the degree of grain-filling plumpness and quality. The calculation formula is

$$\mathrm{BGR}=\frac{DW_{\mathrm{ear}} - DW_{\mathrm{grain}}}{DW_{\mathrm{ear}}} \tag{1}$$

where $DW_{\mathrm{ear}}$ is panicle dry weight (including grains, glumes and rachis) and $DW_{\mathrm{grain}}$ is grain dry weight. BGR ranges from 0 to 1 (dimensionless); lower values indicate plumper grains and better quality. The physiological significance of this index is that the difference between panicle dry weight and grain dry weight reflects the portion of assimilates that failed to be converted into plump grains during filling (including blighted grains, empty glumes and non-grain structures). Under drought stress, reduced filling efficiency directly manifests as an increase in this difference. Therefore, this index not only avoids the subjective errors of water-separation methods, but also quantitatively reflects the efficiency of assimilate transport to grains and the degree of grain plumpness from the perspective of source–sink dynamics.

It should be noted that BGR as defined here differs from the empty grain rate or incompletely filled grain rate measured by traditional wind- or water-separation methods. Wind/water separation methods classify grains based on density differences, primarily identifying empty or incompletely filled grains [18,19]. In contrast, our dry-weight-based BGR captures the total non-grain fraction of the panicle, including glumes, rachises, and unfilled grains, thus reflecting the assimilate loss due to incomplete grain filling from a source–sink dynamics perspective. This distinction is important because BGR provides a quantitative measure of filling efficiency, rather than merely a count-based classification of grain plumpness.

#### 2.3.2. Harvest Index

Harvest index (HI) is calculated as

$$\mathrm{HI} = \frac{DW_{\mathrm{grain}}}{DW_{\mathrm{ear}} + DW_{\mathrm{straw}}} \tag{2}$$

where $DW_{\mathrm{grain}}$ is grain dry weight, $DW_{\mathrm{ear}}$ is panicle dry weight, and $DW_{\mathrm{straw}}$ is stem–leaf dry weight. HI reflects the partitioning of photosynthetic products to the harvested organ (grain), and is an important indicator of source–sink coordination under stress [28].

#### 2.3.3. Drought-Resistance Indices

For the convenience of subsequent index calculations, the following basic parameters are first defined:

$\mathrm{Y_s}$: grain yield of the variety under the current treatment (kg/ha).

$\mathrm{Y_p}$: grain yield of the variety under well-watered treatment (kg/ha).

$\bar{\mathrm{Y}}_{\mathrm{s}}$: average yield of all varieties under the current treatment (kg/ha).

$\bar{\mathrm{Y}}_{\mathrm{p}}$: average yield of all varieties under well-watered treatment (kg/ha).

This study used eight representative traditional drought-resistance indices, covering yield-oriented, stability-oriented and comprehensive types. All indices were calculated based on data from the drought treatment, while indices that involve irrigated yield ($Y_p$) also used well-watered treatment data.

(1) Yield-oriented indices

Drought Yield Index (DYI) reflects the relative yield performance of a variety under drought conditions, proposed by Raman et al. [7]:

$$DYI = \frac{Y_s}{\bar{Y}_s} \tag{3}$$

Mean Productivity (MP): the arithmetic mean yield of a variety under drought and well-watered treatments, reflecting overall productivity [8]:

$$MP = \frac{Y_s + Y_p}{2} \tag{4}$$

Geometric Mean Productivity (GMP): the geometric mean of yields under drought and well-watered treatments, more sensitive to performance in low-yielding environments [9]:

$$GMP = \sqrt{Y_s \times Y_p} \tag{5}$$

(2) Stability-oriented indices

Yield Stability Index (YSI) measures the stability of yield of varieties under drought and irrigated conditions, with larger values indicating better stability [5]:

$$YSI = \frac{Y_s}{Y_p} \tag{6}$$

Drought Stress Susceptibility Index (DSSI) measures the susceptibility of a variety to drought stress, with smaller values indicating lower susceptibility [6]:

$$DSSI = \frac{1 - \frac{Y_s}{Y_p}}{1 - \frac{\bar{Y}_s}{\bar{Y}_p}} \tag{7}$$

(3) Comprehensive indices

Drought-Resistance Index (DRI) comprehensively considers yield performance and stability under drought stress, proposed by Bidinger et al. [10]:

$$DR\,I = \frac{Y_s}{\bar{Y}_s} \times \left(\frac{Y_p}{\bar{Y}_p}\right)^2 \tag{8}$$

Drought Stress Tolerance Index (DSTI) measures the ability of a variety to maintain yield under drought stress [11]:

$$DSTI = \frac{Y_s^2}{Y_p \times \bar{Y}_s} \tag{9}$$

Drought-Resistance Index Difference (DRID) combines DSTI and DSSI to balance yield and stability [11]:

$$DRID = DSTI - DSSI \tag{10}$$

*2.4. Construction of the Yield–Quality Synergy Index (YQSI)*

This study proposes a novel drought-resistance index, the Yield–Quality Synergy Index (YQSI), which is composed of the drought yield index and blighted grain rate. The core design philosophy is first determining the yield potential based on relative yield, then applying a quality penalty through blighted grain rate, thereby achieving the synergistic screening of high yield and good quality. The YQSI is calculated as

$$YQSI = DYI - BGR \tag{11}$$

where DYI is the drought yield index, reflecting the relative yield advantage of a variety under drought compared to the population mean; BGR is the blighted grain rate (0–1) of the variety under the current treatment, directly quantifying the quality loss due to poor grain filling. Subtracting BGR from DYI means deducting the quality discount caused by poor filling from the relative yield advantage; the remainder is the effective yield advantage. This preserves high yield potential, while penalizing varieties with low filling efficiency.

The physiological basis of this construction is that under drought stress, yield level mainly depends on pre-anthesis biomass accumulation and post-anthesis assimilate transport, while BGR directly reflects transport efficiency [17]. A high-yielding variety with poor filling efficiency (high BGR) will have its YQSI value reduced due to the penalty; conversely, a moderate-yielding variety with plump grains (low BGR) may have a higher YQSI value. Thus, the YQSI automatically achieves a trade-off between yield and quality, selecting varieties that excel in both aspects.

To verify the robustness of the simple subtraction formula (YQSI = DYI − BGR), we conducted a comprehensive sensitivity analysis including value range analysis, correlation analysis, and weight sensitivity analysis.

Value range analysis showed that DYI ranged from 0.33 to 2.03 (mean = 1.005, CV = 33.7%), while BGR ranged from 0.26 to 0.66 (mean = 0.414, CV = 18.8%). Both are dimensionless indices (Figure 2). Although DYI has a wider range, the CV of BGR is lower, indicating more concentrated variation.

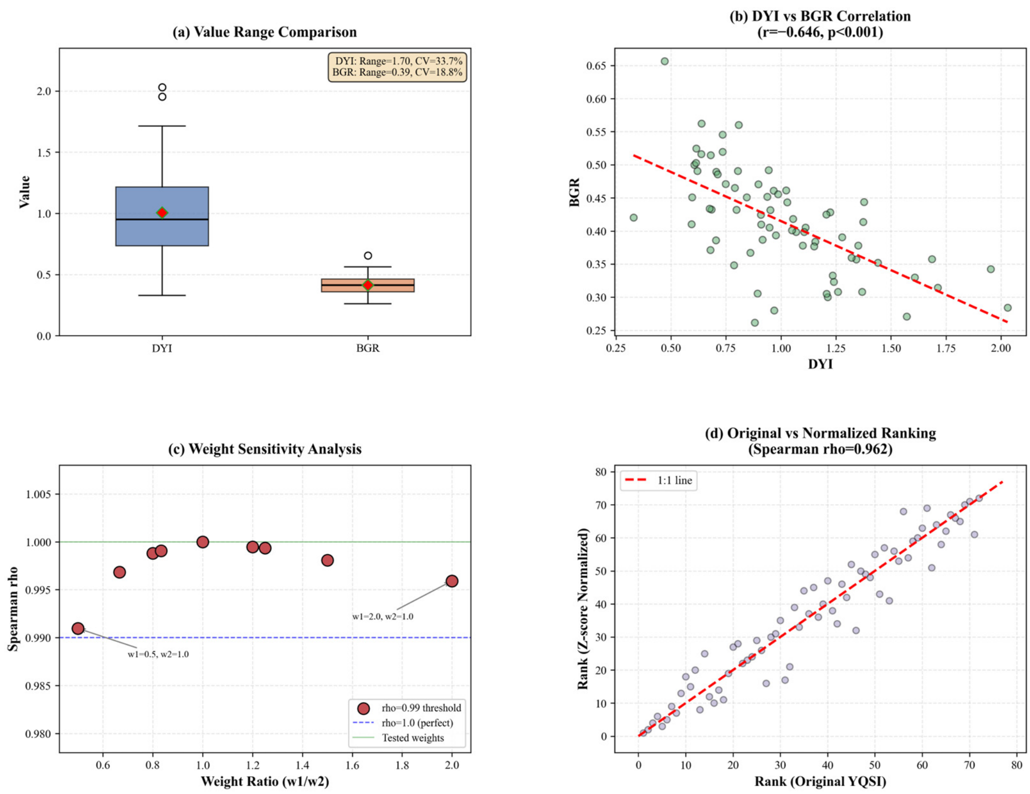


**Figure 2.** Sensitivity analysis of YQSI formula. (**a**) Boxplots of DYI and BGR value ranges; (**b**) scatter relationship between DYI and BGR (r = −0.645); (c) weight sensitivity analysis (weight ratio 0.5–2.0, ϱ > 0.99), where red circles denote Spearman ϱ values, the blue dashed line indicates the ϱ = 0.99 threshold, and the green solid line indicates perfect agreement (ϱ = 1.0) (**d**) rank consistency between original and normalized YQSI (ϱ = 0.962).

Correlation analysis revealed a moderate negative Pearson correlation between DYI and BGR (r = −0.645), indicating that these two metrics capture different dimensions of drought-resistance information, supporting the rationale for their joint use in a single index (Figure 2).

Sensitivity analysis of the formula showed that the absolute sensitivity of the YQSI to both DYI and BGR is identical (dYQSI/dDYI = 1, dYQSI/dBGR = −1) (Figure 2). However, in terms of elasticity, a 1% change in DYI leads to a 1.70% change in the YQSI, while a 1% change in BGR leads to a 0.70% change in the YQSI.

Crucially, a Z-score normalization comparison showed that the Spearman rank correlation between the original YQSI and Z-score-normalized YQSI reached $\rho = 0.962$, indicating that normalization does not alter variety rankings (Figure 2). This proves that the direct subtraction of raw DYI and BGR is mathematically equivalent to subtraction after normalization.

Weight sensitivity analysis provided the strongest evidence: even when the weight assigned to BGR varied from 0.5 to 2.0 (a 4-fold range), the Spearman $\rho$ between the original and weighted YQSI remained > 0.99, and the overlap of top-5 and top-10 varieties remained at 4–5/5 and 9–10/10, respectively. This demonstrates that the rankings are extremely robust to changes in the quality-penalty weight.

### *2.5. Performance Comparison of Drought-Resistance Indices*

To systematically compare the screening performance of the YQSI and eight existing drought-resistance indices, we established a multi-level evaluation system, including methods for variety screening, screening performance evaluation, and annual stability evaluation.

The variety screening method used a reference variety threshold approach, with Yugu 18, a drought-resistant variety widely grown in the North China summer millet region, as the reference. For each index in each year under the drought treatment, varieties with index values greater than those of Yugu 18 (for indices where larger values indicate better drought resistance: YQSI, DYI, DRI, YSI, MP, GMP, DSTI, and DRID) were identified as drought-resistant; for DSSI (where smaller values indicate better drought resistance), varieties with values smaller than that of Yugu 18 were identified as drought-resistant. This method uses a widely adopted drought-resistant variety as a benchmark, so the screening results directly reflect the drought-resistance advantage of varieties relative to a currently promoted variety, providing clear practical guidance.

The screening performance evaluation method used an average ranking approach. To compare the performance of each drought-resistance index in screening varieties with high yield and high harvest index, the following steps were used:

① For a given year (e.g., 2024), for each drought-resistance index, calculate the average yield and average harvest index under drought treatment of all varieties screened by that index.

② Rank the nine drought-resistance indices from highest to lowest average yield to obtain a yield ranking for each index (rank 1 means the highest average yield); similarly, rank the indices from highest to lowest average harvest index to obtain a harvest index ranking for each index.

③ Calculate the average ranking for each index in that year = (yield ranking + harvest index ranking)/2. A smaller value indicates higher screening performance of that index in that year.

④ Repeat the above calculation for 2024 and 2025 separately to obtain the average ranking for each index in both years.

⑤ Finally, the comprehensive ranking of each index = (average ranking in 2024 + average ranking in 2025)/2. A higher ranking (smaller numerical value) indicates that the varieties screened by that index have better comprehensive performance in terms of yield and harvest index, i.e., higher screening performance.

The annual stability-evaluation method used a multi-indicator comprehensive assessment system. Because the experiments were conducted under a rainout shelter with strictly controlled water regimes, the drought treatment received no irrigation throughout the growing season, and concrete water barriers between plots prevented lateral water seepage. Therefore, the differences between the two years mainly originated from natural fluctuations in environmental factors such as light and temperature. Under such conditions, the annual stability of each variety's drought-resistance expression can more purely reflect its genetic stability. Accordingly, we used three indicators: Jaccard similarity, Spearman's rank correlation coefficient, and a composite score, to evaluate the annual screening stability of each drought-resistance index.

Jaccard similarity is a classic statistical indicator for measuring the similarity between two sets, calculated as

$$J(A,B) = \frac{|A \cap B|}{|A \cup B|} \tag{12}$$

where A is the set of superior varieties screened in the first year, and B is the set of superior varieties screened in the second year. The numerator is the number of varieties screened in both years (i.e., truly stable superior varieties), and the denominator is the total number of varieties screened in the two years (excluding duplicates). Jaccard similarity ranges from 0 to 1. Higher values indicate stronger annual repeatability of the screening results. This indicator eliminates the influence of different screening numbers and directly reflects the consistency of screening results.

Spearman's rank correlation coefficient is a non-parametric statistic that measures the monotonic relationship between two variables. It is independent of data distribution assumptions and is insensitive to outliers. It is calculated as

$$\rho = 1 - \frac{6\sum_{i=1}^{n} d_i^2}{n(n^2-1)} \tag{13}$$

where $d_i$ is the difference between the ranks of the varieties in the two years, and n is the number of varieties. In this study, Spearman's rank correlation coefficient is used to calculate the correlation of variety drought-resistance rankings between the two years. Positive values indicate consistent ranking trends across years, negative values indicate opposite trends, and the absolute value indicates the strength of the annual ranking stability. Its absolute value reflects how regularly the index values vary with yield.

The composite score is calculated from the above two indicators and is used to comprehensively rank the annual stability of each drought-resistance index:

$$Score = J(A,B) + \rho \tag{14}$$

The Spearman rank correlation coefficient measures the consistency of variety drought-resistance rankings between the two years. Positive values indicate consistent ranking trends, and the magnitude reflects the strength of the annual ranking stability. A higher composite score indicates stronger annual screening stability. The weighting design follows the principle that Jaccard similarity and Spearman's rank correlation coefficient are equally important, evaluating stability from the two dimensions of screening set and ranking order. A higher composite score indicates stronger annual screening stability of that drought-resistance index.

Through this multi-level evaluation system, we could comprehensively compare the strengths and weaknesses of each drought-resistance index from both screening performance (average ranking method) and annual stability (multi-indicator comprehensive assessment) dimensions, providing a scientific screening tool for foxtail millet drought-resistance breeding.

*2.6. Model Construction and Accuracy Evaluation*

To achieve the goal of screening drought-resistant varieties during the foxtail millet growing season, we used the Random Forest (RF) algorithm to construct a YQSI prediction model. RF can effectively handle non-linear relationships between high-dimensional features and small samples. It has strong resistance to overfitting, is insensitive to outliers, and has good interpretability [29]. It has been widely used in crop phenotypic prediction [23].

First, feature extraction and selection were performed. From UAV RGB, thermal infrared, and multispectral images, we extracted 53 features related to spectrum, texture, temperature and colour (see Appendix A). Specifically, three colour indices (ExG, ExGR, and GRVI) were extracted to characterise canopy greenness and coverage. Seventeen spectral indices (e.g., NDVI, GNDVI, NDRE, EVI2, and SAVI) and 32 texture features (mean, variance, homogeneity, contrast, dissimilarity, entropy, second moment and correlation from the GLCM matrix, applied to the red, green, red-edge and near-infrared bands) were extracted. Spectral indices were used to estimate chlorophyll content, canopy structure and biomass. Texture features were used to reflect canopy structural complexity and spatial heterogeneity. One temperature index (NRCT) was extracted to characterise canopy water status and transpiration efficiency.

Second, the sample set was constructed and divided. A total of 648 samples under three water treatments (NW, DW, and WW) in 2024 and 2025 were included. By introducing different water gradients, sample diversity was effectively expanded, allowing the model to learn a wider range of YQSI variation patterns and thus improve generalization ability. A stratified sampling strategy (stratified by yield type) was used to randomly split the dataset into a training set (453 samples) and a test set (195 samples) with a ratio of 7:3, ensuring that the three water treatments were balanced between the training and test sets.

Finally, modelling parameters were set. The Random Forest model was implemented using the Python scikit-learn library (version 1.2.2). The main hyperparameters were set as follows: n_estimators = 100, max_depth = None, min_samples_split = 2, min_samples_leaf = 1, max_features = sqrt, bootstrap = True, random_state = 42, n_jobs = −1. Other parameters were left at default values.

The final step was model accuracy evaluation. The coefficient of determination ($R^2$) and root mean square error (RMSE) were used to evaluate prediction performance on the test set:

$$R^2 = 1 - \frac{\sum_{i=1}^{n}(y_i - \hat{y}_i)^2}{\sum_{j=1}^{n}(y_j - \bar{y})^2} \tag{15}$$

$$RMSE = \sqrt{\frac{1}{n}\sum_{i=1}^{n}(y_i - \hat{y}_i)^2} \tag{16}$$

$$MAE = \frac{1}{n}\sum_{i=1}^{n}|y_i - \hat{y}_i| \tag{17}$$

where $y_i$ is the measured YQSI value of the i-th sample, $y_j$ is the measured YQSI value of the j-th sample, $\hat{y}_i$ is the YQSI value predicted by the model, $\bar{y}$ is the mean of measured YQSI values, and n is the number of samples.

To evaluate the performance of predicted YQSI in screening drought-resistant varieties, we used the measured YQSI value of the reference variety Yugu 18 as a threshold. Based on measured YQSI and predicted YQSI, varieties were classified as drought-resistant (positive class) or non-drought-resistant (negative class). Based on this binary classification, a confusion matrix was constructed, defining the following four basic quantities.

TP (True Positive): number of samples predicted as drought-resistant that are actually drought-resistant. That is, the model correctly identified drought-resistant varieties.

FP (False Positive): number of samples predicted as drought-resistant but actually non-drought-resistant. That is, varieties misidentified as drought-resistant (false positives).

FN (False Negative): number of samples predicted as non-drought-resistant but actually drought-resistant. That is, drought-resistant varieties missed by the model (false negatives).

TN (True Negative): number of samples predicted as non-drought-resistant that are actually non-drought-resistant. That is, the model correctly excluded non-drought-resistant varieties.

Based on the confusion matrix, four indicators: accuracy, precision, recall and F1 score, were calculated.

$$Accuracy = \frac{TP + TN}{TP + FP + FN + TN} \tag{18}$$

Accuracy reflects the proportion of correct classifications by predicted YQSI.

$$Precision = \frac{TP}{TP + FP} \tag{19}$$

Precision measures the proportion of varieties predicted as drought-resistant that are actually drought-resistant, reflecting the reliability of the model's predictions. Higher precision means fewer false positives.

$$Recall = \frac{TP}{TP + FN} \tag{20}$$

Recall measures the proportion of actual drought-resistant varieties that are correctly identified by the model, reflecting the model's ability to detect drought-resistant varieties. Higher recall means fewer missed detections.

$$F1\text{-}score = 2 \times \frac{Precision \times Recall}{Precision + Recall} \tag{21}$$

The F1 score is the harmonic mean of precision and recall, comprehensively reflecting the screening performance of the model. When both precision and recall are high, the F1 score is also high. If they differ greatly, the F1 score decreases. The F1 score ranges from 0 to 1. Larger values indicate a better balance between precision and recall, i.e., better screening performance.

## 3. Results

### *3.1. Two-Year Yield Differences and Meteorological Conditions*

Analysis of two-year data from the strictly water-controlled rainout shelter experiment showed significant differences in yield and blighted grain rate (BGR) among the three water treatments, and that the environmental stress in 2025 was more severe than in 2024 (Figure 3).

Under the strictly water-controlled rainout shelter experiment, three water gradients (WW, DW, and NW) were set in both 2024 and 2025. The two-year results consistently showed that yield decreased significantly and stepwise with reduced water availability, confirming clear treatment gradients.

In 2024, the average yields under WW, DW and NW were 5348, 4288 and 1694 kg/ha, respectively. Compared with WW, DW and NW had yield reductions of 19.8% and 68.3% ($p < 0.001$). The corresponding BGR values were 0.164, 0.221 and 0.402. The drought treatment had BGR increases of 34.8% and 145.1% compared with the deficit-watered and well-watered treatments ($p < 0.001$).

In 2025, the average yields under WW, DW and NW were 3341, 2437 and 1882 kg/ha, respectively. Compared with WW, DW and NW had yield reductions of 27.0% and 43.7%

($p < 0.01$). The BGR values were 0.310, 0.362 and 0.420. The drought treatment had BGR increases of 16.8% and 35.5% compared with the deficit-watered and well-watered treatments ($p < 0.01$).

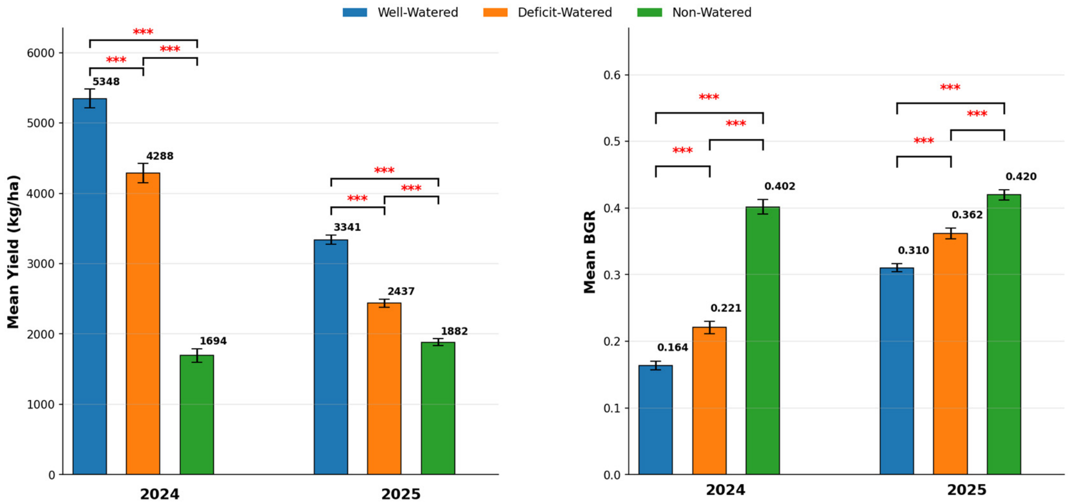


**Figure 3.** Distribution of yield and BGR across all treatments in the two years. *** $p < 0.001$. $n = 72$ (2024) and $n = 144$ (2025) per treatment.

The two-year data fully demonstrate that the water gradient design successfully established an effective stress series from full irrigation to extreme drought, providing good sample variability for subsequent drought-resistance index comparisons and model construction.

### *3.2. Relationship Between Bgr, Yield and Harvest Index*

Based on field measurement data of 48 foxtail millet varieties (drought treatment) from 2024–2025, the varieties were sorted from low to high yield under drought treatment, and statistical trends of BGR versus yield and harvest index were prepared (Figure 4). The results showed that BGR varied considerably among varieties, ranging from 27.1% to 56.2%, with an average of 33.3%. In 2025, Gigu 46 had the lowest BGR (27.1%) and a relatively high drought-treatment yield (2958 kg/ha). Jijinmiao 6 had a BGR of 28.4% and the highest yield (3821 kg/ha). Changnong 47 had the highest BGR (56.2%) and a low yield of 1202 kg/ha. The overall trend indicated that varieties with lower BGR tended to have higher yield potential (Figure 4).

Despite the overall negative correlation, there were counterexamples that deviated from this pattern. Some high-yielding varieties exhibited high blighted grain rates. In 2024, Zhangzagu 18 (2307 kg/ha, ranked fifth in yield) had a BGR as high as 0.444, significantly higher than the year's average of 0.405, whereas the highest-yielding variety that year, Zhangzagu 16 (3272 kg/ha), had a BGR of only 0.343. In 2025, Zhangzagu 22 (2584 kg/ha, ranked fourth in yield) had a BGR of 0.414, significantly higher than Gigu 39 (0.308) at a similar yield level. Zhonggu 303-I (1520 kg/ha, medium-high yield) had a BGR as high as 0.560. On the other hand, some low-yielding varieties had relatively low BGR. In 2024, Zhonggu 19 (1622 kg/ha, below average) had a BGR of only 0.280, and Chigu K10 (1475 kg/ha, ranked 15th) had a BGR as low as 0.262 (the lowest that year). In 2025, Jigu 20 (1328 kg/ha, relatively low) had a BGR of 0.400, slightly below the year's average of 0.420. These counterexamples indicate that yield alone cannot accurately determine grain-filling plumpness. High-yielding varieties may have filling defects, while low- to medium-yielding varieties may still achieve plump grains.

Further analysis of the relationship between BGR and harvest index (HI) showed that higher BGR (poorer grain plumpness) was associated with lower efficiency of photosynthetic-product transport to grains, ultimately leading to a lower harvest index (Figure 4). For example, Jijinmiao 6 (BGR = 0.284, HI = 0.339) performed well in 2025. This further confirms the validity of BGR as a key indicator of grain-filling efficiency. There were also varieties that deviated from this trend. In 2024, Zhangzagu 22 had a BGR of 0.3577 (above average) but a HI as high as 0.3104 (the highest that year). In 2025, Zhangzagu 22 again showed a similar pattern (BGR = 0.4138, HI = 0.259, significantly higher than expected for its BGR level). This suggests that this variety has a high capacity to allocate photosynthetic products to grains (high economic coefficient), but grain-filling plumpness is not ideal, further confirming the trade-off between yield and quality.

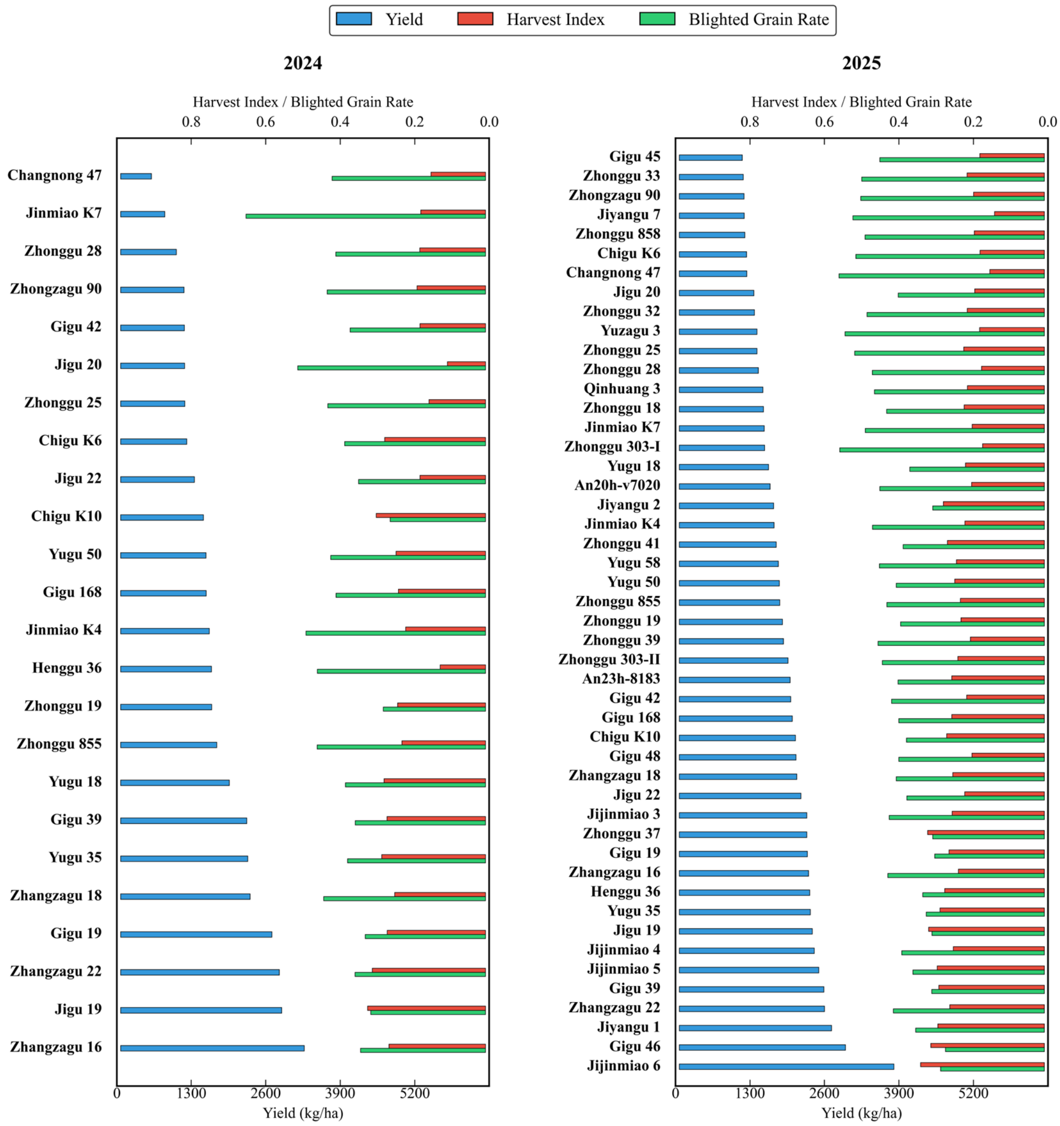


**Figure 4.** Relationship between BGR, yield and harvest index under drought treatment (2024–2025). Varieties are sorted from low to high yield under drought treatment.

### *3.3. Performance Comparison of Different Drought-Resistance Indices in Variety Screening*

The nine drought-resistance indices were calculated for all varieties. Using Yugu 18 as the reference, varieties outperforming Yugu 18 were considered drought-resistant. The numbers of drought-resistant varieties screened by each index and their performance are

https://doi.org/10.3390/agriculture16161765

shown in Table 1. In 2024, YQSI, DYI, DRI, GMP, DSTI and MP each screened seven varieties; YSI and DSSI screened 10 varieties; and DRID screened 16 varieties. In 2025, YQSI, DYI, DRI, GMP, DSTI and MP each screened 31 varieties; YSI and DSSI screened 37 varieties; and DRID screened 15 varieties.

**Table 1.** Number of varieties screened by each drought-resistance index and their comprehensive performance in 2024 and 2025.

| Index | 2024 | | | 2025 | | |
|---|---|---|---|---|---|---|
| | Number Screened | Average Yield (kg/ha) | Average Harvest Index | Number Screened | Average Yield (kg/ha) | Average Harvest Index |
| YQSI | 7 | 2640 | 0.2817 | 31 | 2185 | 0.2013 |
| DYI | 7 | 2640 | 0.2817 | 31 | 2185 | 0.2013 |
| DRI | 7 | 2640 | 0.2817 | 31 | 2165 | 0.2020 |
| GMP | 7 | 2640 | 0.2817 | 31 | 2165 | 0.1996 |
| DSTI | 7 | 2640 | 0.2817 | 31 | 2165 | 0.1996 |
| MP | 7 | 2468 | 0.2718 | 31 | 2151 | 0.1991 |
| DSSI | 10 | 2295 | 0.2697 | 37 | 2005 | 0.1919 |
| YSI | 10 | 2295 | 0.2697 | 37 | 2005 | 0.1919 |
| DRID | 16 | 1277 | 0.1992 | 15 | 1365 | 0.1550 |

Based on the two-year average rankings, the comprehensive ranking of the indices was as follows: YQSI and DYI tied for first, DRI was third, GMP and DSTI tied for fourth, MP was sixth, YSI and DSSI tied for seventh, and DRID was ninth. This indicates that YQSI performs comparably to the best traditional indices in balancing yield and harvest index, while additionally incorporating grain quality information through the BGR penalty, which no traditional index provides.

To further address the concern that different indices may select different numbers of varieties, thereby affecting mean performance comparisons, we conducted a top-k consistency analysis using a common selection proportion. For 2024, we set k = 7 (the number selected by most indices, including YQSI, DYI, DRI, DRID, DSTI and GMP); for 2025, we set k = 31 (the number selected by seven indices, including YQSI, DYI, DRI, DRID, DSTI, GMP and MP). Under this unified threshold, we recalculated the average yield, harvest index (HI), and blighted grain rate (BGR) of the varieties selected by each index (Table 2).

**Table 2.** Top-k consistency analysis: average performance of selected varieties under a unified selection proportion (2024: k = 7; 2025: k = 31).

| Index | 2024 (k = 7) | | | 2025 (k = 31) | | |
|---|---|---|---|---|---|---|
| | Yield (kg/ha) | HI | BGR | Yield (kg/ha) | HI | BGR |
| YQSI | 2640 | 0.4518 | 0.3605 | 2185 | 0.2571 | 0.3771 |
| DYI | 2640 | 0.4518 | 0.3605 | 2185 | 0.2571 | 0.3771 |
| DRI | 2640 | 0.4518 | 0.3605 | 2165 | 0.2548 | 0.3869 |
| DRID | 2640 | 0.4518 | 0.3605 | 2165 | 0.2548 | 0.3869 |
| DSTI | 2640 | 0.4518 | 0.3605 | 2164 | 0.2546 | 0.3827 |
| GMP | 2640 | 0.4518 | 0.3605 | 2164 | 0.2546 | 0.3827 |
| MP | 2468 | 0.4311 | 0.3494 | 2151 | 0.2543 | 0.3856 |
| YSI | 2536 | 0.4478 | 0.3674 | 2069 | 0.2448 | 0.4003 |
| DSSI | 1010 | 0.3105 | 0.4505 | 1721 | 0.2222 | 0.4340 |

The top-k analysis yielded three key findings. Under a unified selection proportion, YQSI and DYI consistently ranked first in both years in terms of average yield and HI, followed by DRI, DRID, DSTI, and GMP, with MP, YSI, and DSSI trailing behind. This pattern is fully consistent with the results obtained using the reference-variety threshold method (Table 1), confirming that our core conclusions are robust to differences in selection numbers.

Meanwhile, based on the two-year data, we calculated the nine indices for the 24 varieties in 2024 and ranked them, and did so similarly for the 48 varieties in 2025. We then produced heatmaps of the rankings for each variety in each year (Figure 5). For each variety, we averaged its rankings across the indices (for DSSI, smaller values give better rankings; for all other indices, larger values give better rankings) to obtain a comprehensive drought-resistance ranking. Higher comprehensive ranking indicates stronger drought resistance, and in the heatmap this is shown by greener (lighter) colours and a position closer to the top.

We found that among the top 10 comprehensive rankings in 2024 and the top 10 in 2025, most indices identified Zhangzagu 16 (2024) and Jijinmiao 6 (2025) as drought-resistant varieties. In 2024, YQSI and DYI had the highest accuracy (10/10), in that the varieties they ranked in the top 10 were exactly those that were among the comprehensive top 10. In 2025, YQSI, DRI, DRID and DYI had the highest accuracy (9/10), in that the varieties they ranked in the top 10 were among the comprehensive top 10.

Although the selected germplasm set was identical, the internal ranking differed substantially among indices. To illustrate this, we examined the top seven varieties within this common set (2025), which represent the most elite germplasms identified by all six indices (Table 3).

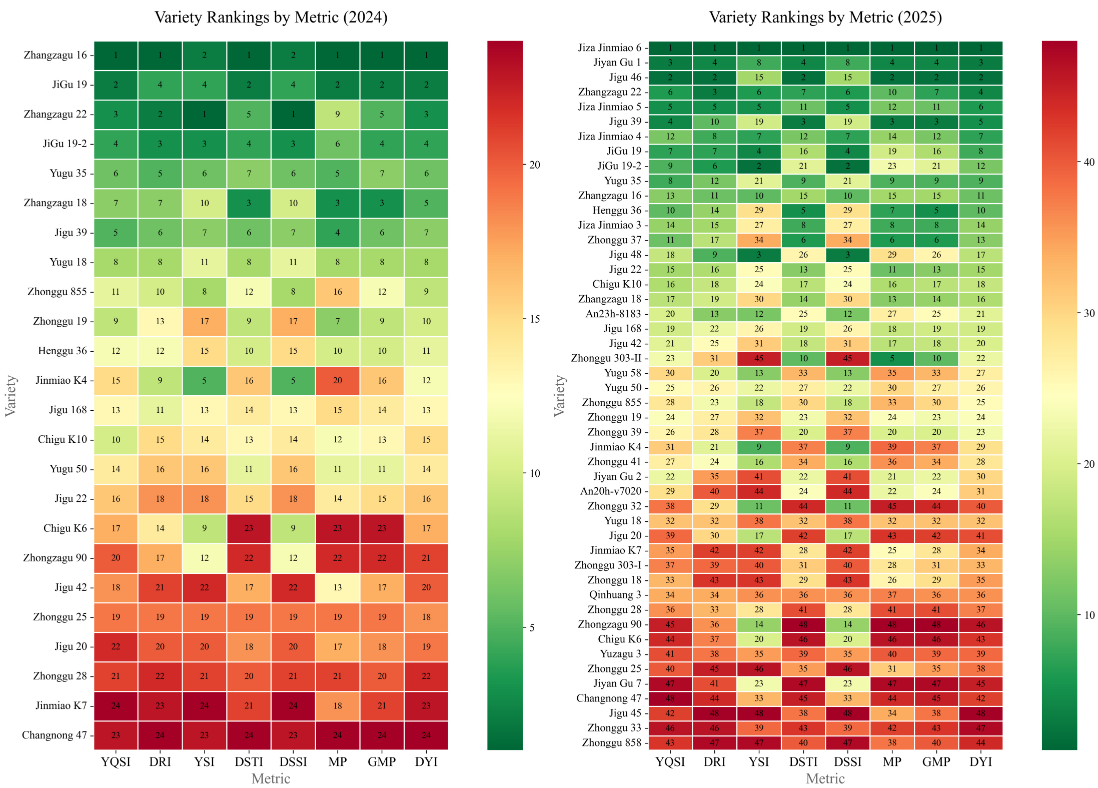


**Figure 5.** Heatmaps of variety drought-resistance rankings for each index in the two years. Numbers in each cell represent the rank of that variety under the corresponding index. Greener (lighter) colours indicate higher rankings (stronger drought resistance), and darker (redder) colours indicate lower rankings (weaker drought resistance).

**Table 3.** Internal ranking of the same top seven varieties (2025) under six indices and independent quality traits.

| Variety | Ranking Under Each Index | | | | | | Trait Values | | |
|---|---|---|---|---|---|---|---|---|---|
| | YQSI | DYI | DRI | DRID | DSTI | GMP | BGR | Yield (kg/ha) | HI |
| Gigu 39 | 1 | 2 | 4 | 2 | 1 | 1 | 0.308 | 171.74 | 0.289 |
| Zhangzagu 22 | 2 | 1 | 1 | 1 | 3 | 3 | 0.414 | 172.28 | 0.259 |
| Jigu 19 | 3 | 3 | 3 | 3 | 6 | 6 | 0.308 | 157.98 | 0.317 |
| Yugu 35 | 4 | 4 | 6 | 6 | 4 | 4 | 0.323 | 155.49 | 0.286 |
| Gigu 19 | 5 | 7 | 2 | 4 | 7 | 7 | 0.300 | 152.07 | 0.261 |
| Henggu 36 | 6 | 5 | 7 | 7 | 2 | 2 | 0.333 | 154.95 | 0.273 |
| Zhangzagu 16 | 7 | 6 | 5 | 5 | 5 | 5 | 0.429 | 153.51 | 0.235 |

Despite the identical selected set, the internal rankings varied considerably across indices. The YQSI upgraded Gigu 39 from second (under DYI) to first due to its superior BGR (0.308), while downgrading Zhangzagu 22 from first (under DYI) to second because of its high BGR (0.414). Similarly, Gigu 19 rose from seventh under DYI to fifth under the

YQSI, owing to its low BGR (0.300). These re-rankings demonstrate that the YQSI does not merely replicate DYI screening outcomes; it applies a biologically meaningful quality penalty that reorders varieties within the same elite group based on independently measured grain-filling performance (BGR).

### 3.4. Annual Stability of Drought-Resistance Index Screening

To evaluate the stability and repeatability of screening results across years for different drought-resistance indices, we systematically compared the varieties screened by each index in 2024 and 2025. In 2024, 24 varieties were tested; in 2025, 48 varieties were tested, of which 24 were the same as in 2024. To evaluate annual stability and avoid interference from differences in variety composition, the following analysis is based only on the 24 varieties that were used in both years.. Table 4 shows the screening results for each index calculated, based only on these 24 common varieties. The numbers and composition of varieties screened by each index varied between the two years.

In terms of Spearman's rank correlation coefficient, all indices showed positive correlations (Table 4), indicating that the drought-resistance rankings of varieties were generally consistent between the two years, despite differences in environmental conditions. The YQSI achieved the highest Spearman ϱ (0.823), followed by DRI (0.796) and DYI (0.783). Notably, the YQSI and DYI do not rely on well-watered yield, which contributes to their higher rank consistency across years. DSSI, despite having a relatively high Spearman ϱ (0.758), screened only two common varieties between the two years, resulting in the lowest composite score (0.912).

**Table 4.** Annual screening stability of each drought-resistance index based on common varieties (24) (2024 vs. 2025 common varieties).

| Index | Number Screened in 2024 | Number Screened in 2025 (Based on Common 24) | Number Screened in Both Years | Jaccard Similarity | Spearman ϱ | Composite Score |
|---|---|---|---|---|---|---|
| YQSI | 7 | 16 | 7 | 0.438 | 0.823 | 0.781 |
| YSI | 10 | 21 | 10 | 0.476 | 0.758 | 0.675 |
| DRI | 7 | 17 | 7 | 0.412 | 0.796 | 0.725 |
| DRID | 7 | 18 | 7 | 0.389 | 0.775 | 0.632 |
| DYI | 7 | 16 | 7 | 0.438 | 0.783 | 0.751 |
| MP | 7 | 16 | 7 | 0.438 | 0.743 | 0.740 |
| DSTI | 7 | 16 | 7 | 0.438 | 0.737 | 0.698 |
| GMP | 7 | 16 | 7 | 0.438 | 0.737 | 0.698 |
| DSSI | 13 | 2 | 2 | 0.154 | 0.758 | 0.353 |

Using Yugu 18 as the reference, each index screened different numbers of drought-resistant varieties in the two years. We counted the varieties that were screened in both years (Table 5). The results showed that YQSI, DRI, DRID, DYI, DSTI and GMP screened exactly the same set of varieties in both years (seven varieties each). Among them, the common varieties screened by the YQSI had an average yield of 2640 kg/ha and a harvest index of 0.282 in 2024; in 2025, the average yield was 2363 kg/ha and the harvest index was 0.213. These values were significantly superior to the common varieties screened by YSI, MP and DSSI. DSSI had only two common varieties between the two years, and their yield (966 kg/ha in 2024, 1448 kg/ha in 2025) and harvest index (0.166 in 2024, 0.169 in 2025) were significantly lower than those of the other indices.

**Table 5.** Performance of the varieties screened by each index in both years.

| Index | Average Yield of Common Varieties in 2024 (kg/ha) | Average Yield of Common Varieties in 2025 (kg/ha) | Average HI of Common Varieties in 2024 | Average HI of Common Varieties in 2025 |
|---|---|---|---|---|
| YQSI | 2640 | 2363 | 0.282 | 0.213 |
| YSI | 2295 | 2121 | 0.270 | 0.200 |
| DRI | 2640 | 2363 | 0.282 | 0.213 |
| DRID | 2640 | 2363 | 0.282 | 0.213 |
| DYI | 2640 | 2363 | 0.282 | 0.213 |
| MP | 2468 | 2256 | 0.272 | 0.210 |
| DSTI | 2640 | 2363 | 0.282 | 0.213 |
| GMP | 2640 | 2363 | 0.282 | 0.213 |
| DSSI | 966 | 1448 | 0.166 | 0.169 |

It is noteworthy that, although the YQSI and indices such as DYI and DRI screened exactly the same common varieties in both years, the composite score of the YQSI (1.261) was higher than that of DYI (1.221) and DRI (1.208). This is because the YQSI incorporates BGR into its calculation, optimising the ranking of varieties and making the screening results more aligned with the breeding goal of high yield and good quality. Compared with YSI, the YQSI had a slightly lower Jaccard similarity, but the stable varieties screened by the YQSI were agronomically superior, indicating that the YQSI maintains good annual repeatability while pursuing quality constraints.

In summary, the YQSI index can effectively identify drought-resistant varieties that are stable across years, and these stable varieties perform excellently in terms of yield and harvest index. The six strongly drought-resistant candidate germplasms identified in this study (Gigu19, Gigu 39, Zhangzagu 18, Zhangzagu 16, Yugu 35 and Jigu 19) can be prioritised for drought-resistance breeding and production promotion in arid areas.

### *3.5. Accuracy of Yqsi Prediction*

Based on the Random Forest algorithm, the YQSI index was predicted using UAV multimodal data. The model performed excellently on the test set (195 samples): $R^2$ = 0.8193, MAE = 0.1346, RMSE = 0.1741 (Figure 6). The mean prediction error was 0.0201 and the standard deviation was 0.1734, indicating no systematic bias. Using ±0.3 as a threshold, 173 samples (88.7%) were normal and 22 samples (11.3%) were outliers.

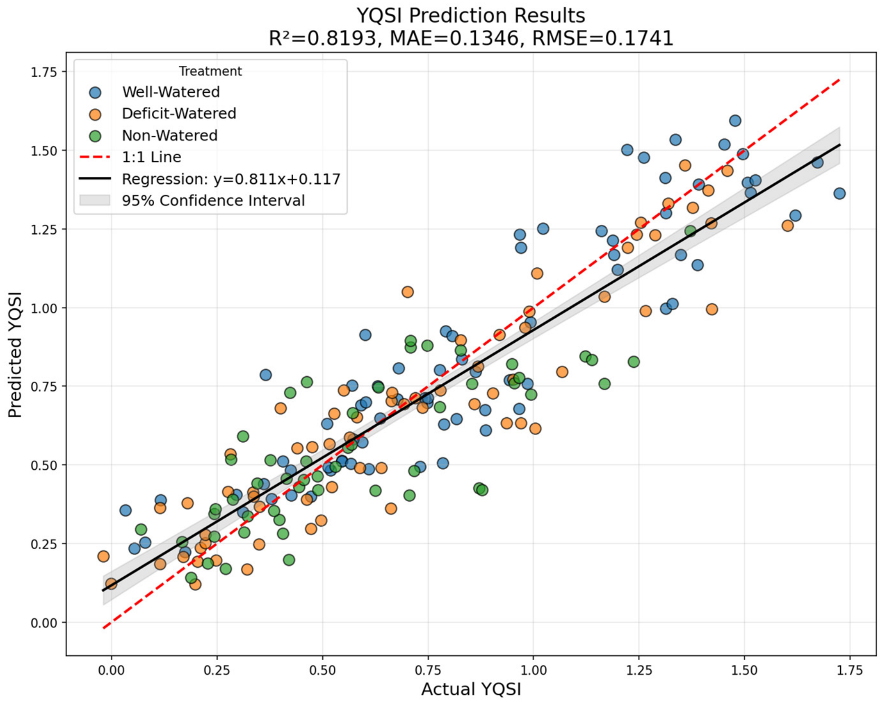


**Figure 6.** Scatter plot of predicted vs. measured YQSI values based on UAV multimodal data on the test set. The dashed line represents the 1:1 line. Shaded area indicates the 95% confidence interval.

Analysis by water treatment (Table 6) showed that the deficit-watered treatment had the highest accuracy ($R^2$ = 0.8457), followed by the well-watered treatment ($R^2$ = 0.8235), and the drought treatment had relatively lower but still acceptable accuracy ($R^2$ = 0.6140). The overall $R^2$ = 0.8193 indicates that the model has acceptable predictive ability. The inclusion of multiple water treatments effectively enhanced sample diversity, enabling the model to maintain good predictive ability under different water conditions and significantly improving generalisation.

**Table 6.** YQSI test set accuracy under different water treatments.

| Water Treatment | Sample Size | $R^2$ | RMSE | MAE |
|---|---|---|---|---|
| Non-Watered | 54 | 0.6140 | 0.1931 | 0.1500 |
| Deficit-Watered | 68 | 0.8457 | 0.1598 | 0.1259 |
| Well-Watered | 73 | 0.8235 | 0.1803 | 0.1433 |

Analysis of the 5% of samples with the largest absolute prediction errors (10 samples, 5.1% of the test set) (Figure 7) revealed two main types. First, high-YQSI varieties were underestimated. Examples include Chigu K10 (drought treatment, measured YQSI = 0.8704, predicted YQSI = 0.4270, error + 0.4434) and Jijinmiao 4 (drought treatment, measured YQSI = 0.8777, predicted YQSI = 0.4211, error + 0.4567). This may be because rapid canopy senescence during late filling reduced greenness while the filling process was still ongoing, causing a mismatch between spectral features and YQSI dynamics. Second, low-YQSI varieties were overestimated. Examples include Gigu 42 (well-watered treatment, measured YQSI = 0.3646, predicted YQSI = 0.7873, error − 0.4227) and Zhonggu 25 (deficit-watered treatment, measured YQSI = 0.7008, predicted YQSI = 1.0511, error − 0.3503). These varieties may exhibit abnormal spectral features such as premature canopy senescence or leaf rolling. Overall, the proportion of outliers was low, indicating that the model has stable and reliable predictive ability for the vast majority of varieties.

The overall $R^2$ = 0.8193 indicates that the model has good predictive ability across the combined dataset. The $R^2$ of 0.614 under the non-watered treatment, while lower than under other treatments, is comparable to, or exceeds, values reported in similar UAV-based drought-resistance prediction studies, and is acceptable for early-stage breeding screening where the primary goal is to rank varieties, rather than to achieve absolute yield prediction accuracy.

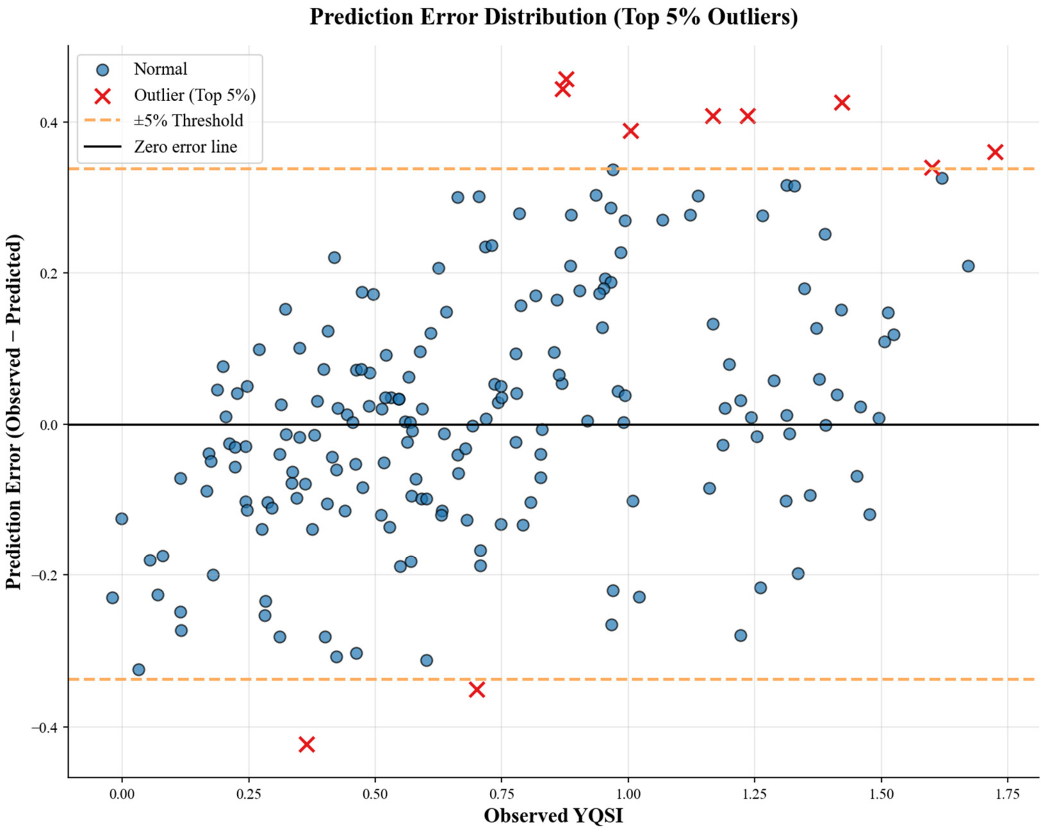


**Figure 7.** Prediction error distribution and representative outlier samples. The dashed lines indicate ±5% error thresholds.The black solid line indicates zero prediction error.

To identify the key remote sensing variables influencing YQSI prediction, we conducted a feature-importance analysis based on the Random Forest model (Figure 8). The top 20 features accounted for approximately 53.9% of the total importance. NDVI was the most important feature (5.88%), followed by WDRVI (5.43%) and RE_MEA (5.38%). The top five features (NDVI, WDRVI, RE_MEA, NRCT, and RVI) contributed approximately 26.5% of the total importance.

Notably, both vegetation indices (e.g., NDVI, WDRVI and RVI) and texture features (e.g., RE_MEA and NIR_COR) played important roles, indicating that integrating spectral and textural information is essential for accurate YQSI prediction. The canopy temperature index (NRCT, ranked fourth, 5.05%) was also among the top features, confirming the importance of thermal information for drought-resistance assessment.

https://doi.org/10.3390/agriculture16161765

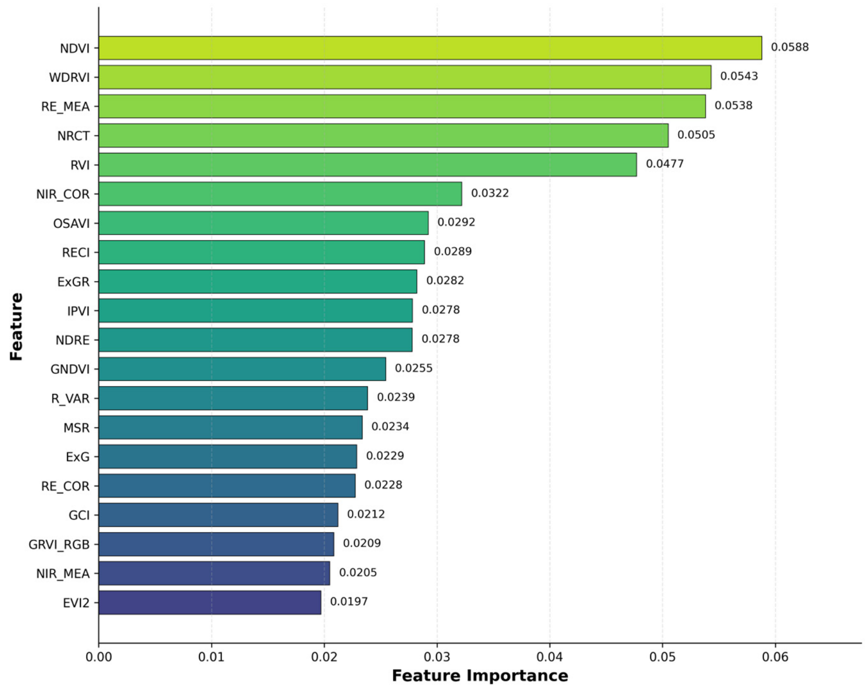


**Figure 8.** Top 20 feature-importance ranking for YQSI prediction based on Random Forest.

### *3.6. Comparison of Drought-Resistant-Variety Screening Based on Predicted vs. Measured Yqsi*

To comprehensively evaluate the performance of predicted YQSI in screening drought-resistant varieties, we systematically analysed the prediction results from two dimensions: variety ranking consistency and screening accuracy. Based on the full drought-treatment samples in 2024 and 2025, using the screening criterion of Yugu 18 as reference (YQSI > reference value), we identified predicted drought-resistant varieties and true drought-resistant varieties based on predicted YQSI and measured YQSI, respectively, and calculated the Spearman rank correlation coefficient and screening performance indicators (accuracy, precision, recall, and F1 score).

The Spearman rank correlation coefficient between predicted YQSI and measured YQSI for all drought-treatment samples was calculated (Figure 9). The results showed that in 2024, Spearman $\varrho = 0.821$ ($p = 0.0234$), and in 2025, Spearman $\varrho = 0.891$ ($p = 2.20 \times 10^{-10}$). Both were significant or highly significant. This indicates that the predicted values and measured values are highly consistent in ranking the drought resistance of varieties, accurately reflecting the relative differences in drought resistance among varieties. The correlation was even stronger in 2025 ($\varrho$ close to 0.9), suggesting that the model performs more robustly with a larger sample size.

Based on the above screening criteria, we counted the numbers of drought-resistant varieties identified by predicted YQSI and measured YQSI and their overlap, and calculated accuracy, precision, recall and F1 score (Table 7). Using Yugu 18 as the reference, varieties outperforming it were identified. In 2024, the measured YQSI identified seven drought-resistant varieties, the predicted YQSI identified eight, and the overlap was seven. The screening accuracy of the prediction was 96.0%, precision was 87.5%, recall was 100%, and the F1 score was 0.933. In 2025, the measured YQSI identified 31 drought-resistant varieties, the predicted YQSI identified 29, and the overlap was 28. The screening accuracy of the prediction was 91.7%, precision was 96.6%, recall was 90.3%, and the F1 score was 0.933.

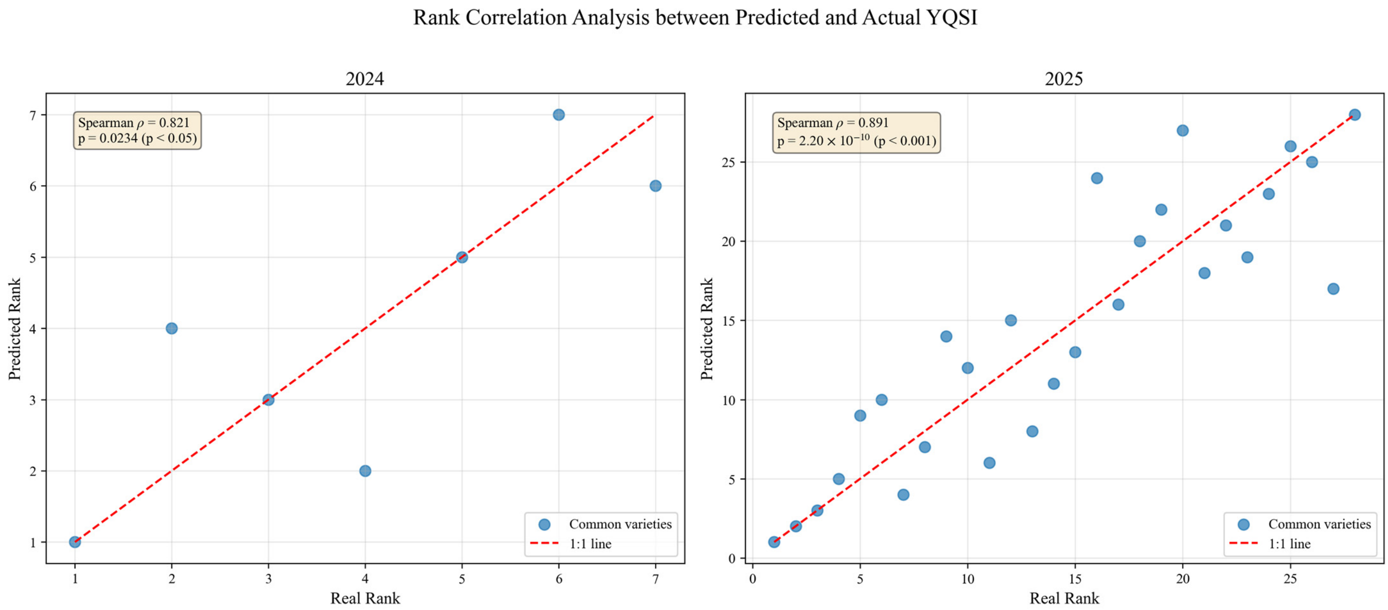


**Figure 9.** Rank correlation of foxtail millet varieties based on predicted vs. measured YQSI rankings. Blue circles represent varieties selected by both predicted and actual YQSI.

**Table 7.** Performance comparison of predicted YQSI versus actual YQSI in screening drought-resistant varieties.

| Year | Number Predicted | Number True | TP | FP | FN | TN | Accuracy | Precision | Recall | F1 Score |
|---|---|---|---|---|---|---|---|---|---|---|
| 2024 | 8 | 7 | 7 | 1 | 0 | 17 | 0.960 | 0.875 | 1.000 | 0.933 |
| 2025 | 29 | 31 | 28 | 1 | 3 | 16 | 0.917 | 0.966 | 0.903 | 0.933 |

Notably, the F1 score was the same in both years (0.933), but the compositions differed. In 2024, recall reached a perfect 100% (all true drought-resistant varieties were identified by the prediction model, no misses), while precision was 87.5% (one false positive among the eight predicted varieties). In 2025, precision reached 96.6% (only one false positive among the 29 predicted varieties), and recall was 90.3% (three true drought-resistant varieties were missed). The identical F1 score indicates that the model achieved different but equivalent balances between no misses and no false positives. Overall, the F1 score exceeded 0.93 in both years, indicating that the prediction model has very high screening reliability under full drought-treatment conditions.

Combining the high consistency in variety ranking (Spearman $\rho > 0.82$, $p < 0.05$) and the excellent screening performance (F1 = 0.933), we conclude that the Random Forest model based on UAV multimodal remote sensing can effectively predict the YQSI index under drought-treatment conditions for the purpose of variety screening. The predicted values maintain a strong positive correlation with measured values in variety ranking and achieve high accuracy and recall in screening drought-resistant varieties. However, validation in independent years, locations, and germplasm populations is needed before the model can be proposed as a general breeding-screening tool.

## 4. Discussion

### *4.1. Advantages of YQSI in Balancing Yield and Quality in Drought-Resistance Screening*

The core innovation of the Yield–Quality Synergy Index (YQSI) proposed in this study is the introduction of blighted grain rate (BGR) as a quality-penalty term into the drought-resistance evaluation system, thereby achieving the synergistic screening of yield and quality. Traditional drought-resistance indices, whether yield-oriented (DYI, MP, and GMP), stability-oriented (YSI and DSSI), or comprehensive (DRI, DSTI, etc.), all use yield as the core evaluation criterion [6–12]. Although these indices have played important roles in drought-resistance screening in various crops [6–12,14], their common drawback is ignoring the profound impact of drought stress on quality.

However, the impact of drought stress on crops is multidimensional. It not only reduces grain number, but also inhibits the transport efficiency of assimilates to grains during grain filling, leading to reduced grain plumpness [16]. The key finding of this study is that yield and BGR are partially decoupled across varieties. High yield does not necessarily imply plump grains, and vice versa (Figure 4). This finding implies that any yield-oriented drought-resistance index may misclassify high-yielding but poor-grain-filling varieties as drought-resistant, while overlooking genotypes with moderate yield but superior filling efficiency. By introducing BGR as a quality-penalty term, YQSI is designed not to pursue mathematical optimality, but to directly address the practical breeding question of how to eliminate filling-defective varieties while maintaining yield potential.

It should be noted that the BGR defined in this study differs in connotation from the empty grain rate determined by traditional wind or water separation methods. Wind or water separation classifies grains based on density differences, and is essentially a count-based indicator. In contrast, BGR captures the mass proportion of total non-grain components of the panicle, quantifying assimilate loss due to incomplete grain filling from a source–sink dynamics perspective. This distinction is agronomically significant. BGR not only reflects grain plumpness itself, but also integrates information on the allocation of assimilates to glumes and rachises, thereby providing a more comprehensive measure of carbon-assimilate partitioning efficiency during grain filling. This is conceptually consistent with the image-based blighted-grain identification method proposed by Liu et al. [18,19], but the dry-weight method used here is better suited for batch measurement in field settings.

Concerning the robustness of the YQSI formula, the sensitivity analysis provides three lines of evidence. First, DYI and BGR show a moderate negative correlation ($r = -0.645$), indicating that these two metrics capture different dimensions of drought-resistance information. DYI reflects relative yield advantage, while BGR reflects filling efficiency. Their direct subtraction is therefore reasonable in information-theoretic terms, rather than being a simple dimensional mismatch. Second, Z-score normalization comparison shows that the variety rankings of original YQSI and normalized YQSI are highly consistent ($\varrho = 0.962$), demonstrating that the range difference between DYI and BGR does not materially affect rank order. Third, and most importantly, even when the penalty weight on BGR varies over a four-fold range, variety rankings remain highly stable ($\varrho > 0.99$), with the overlap of the top-five and top-ten varieties remaining virtually unchanged. This result implies that YQSI rankings are insensitive to weight selection. Breeders need not worry that subjective weight choices will distort screening outcomes. This directly addresses a core concern in breeding practice: if an index requires weight adjustment for different germplasm populations, its objectivity and repeatability will be substantially compromised. The simplicity of the subtraction formula is not a weakness, but an advantage, in this context.

Furthermore, although the YQSI and DYI identified identical numbers of varieties in both years, the YQSI introduced meaningful internal re-ranking through the BGR penalty. Taking 2024 as an example, Zhangzagu 18 ranked fifth under DYI but was downgraded to seventh under the YQSI, due to its BGR of 0.444, the highest among the selected group. Conversely, Gigu 39 ranked seventh under DYI, but was upgraded to fifth under the YQSI because of its relatively moderate BGR, of 0.357. The biological significance of this re-ranking is that it directly reflects varietal differences in filling efficiency, and these differences correspond to independently measured grain quality data. In other words, the YQSI does not simply subtract a constant from DYI, but applies differentiated quality penalties based on each variety's actual filling performance. From a breeding perspective, the value of this internal re-ranking lies in the following. When breeders make choices among varieties with similar yield levels, the YQSI provides a basis for differentiation based on filling quality, which traditional yield-oriented indices cannot offer.

The inter-annual stability of the YQSI further supports its practical value. After correction of the calculation error, the Spearman $\varrho$ of YQSI for two-year variety ranking was 0.823, the Jaccard similarity coefficient was 0.438, and the composite score (1.261) was the highest among all nine indices. This means that the YQSI not only selects similar sets of varieties across years (Jaccard = 0.438, comparable to DYI), but also maintains more stable relative rankings among varieties ($\varrho$ = 0.823, higher than DYI at 0.783 and DRI at 0.796). For breeding practice, the stability of ranking order is more important than the stability of the selected set, because it determines whether breeders can confidently infer varietal relative advantages from single-year data. Methodologically, this study used the widely cultivated variety Yugu 18 as the screening benchmark. Yugu 18 is a leading variety in the Huang–Huai–Hai summer millet region. Using it as a reference means that screening results directly reflect the drought-resistance advantage of test varieties relative to a currently promoted production variety, rather than abstract statistical rankings.

### *4.2. Physiological Basis and Environmental Adaptability of Yqsi-Screened Drought-Resistant Varieties*

The design logic of YQSI is first to determine yield potential and then to screen for quality. The core is to subtract the penalty for blighted grain (BGR) from the relative yield advantage (DYI), which essentially quantifies the efficiency of carbon-assimilate transport to grains and conversion to starch. From a physiological perspective, filling efficiency depends on two key processes: the transport efficiency of photosynthetic assimilates (as sucrose) from source organs to grains, and the synthesis efficiency of converting sucrose into starch for accumulation in grains [17]. Drought stress disrupts both processes, leading to poor grain plumpness and an increased blighted grain rate [16]. The negative correlation between BGR and harvest index observed in this study (Figure 4) confirms that BGR is a key indicator of the efficiency of photosynthetic-product allocation to grains. Therefore, by penalizing varieties with high BGR, YQSI essentially selects genotypes that maintain efficient assimilate transport and starch synthesis under drought, consistent with the source–sink dynamics framework proposed by Yang and Zhang [17]. This physiological interpretation is also supported by the observation that YQSI-selected varieties maintained significantly higher harvest index under drought than varieties selected by other indices (Table 1), indicating superior dry-matter partitioning to the harvested organ.

Vadez et al. [21] emphasized that ensuring water supply during grain filling is crucial for yield formation, because grain filling depends on current photosynthesis and remobilization of pre-anthesis reserves. Under drought stress, the ability to maintain assimilate supply and conversion becomes the primary determinant of both yield and quality. Varieties with high YQSI values, such as Gigu 19 and Zhangzagu 16, likely possess superior water-regulation mechanisms, enabling them to maintain more favourable canopy temperature (as reflected by NRCT, ranked fourth in feature importance) and higher photosynthetic efficiency during grain filling, thus ensuring a continuous supply and efficient conversion of filling assimilates. This is consistent with the findings of Wu et al. [27] that canopy temperature is a reliable indicator of drought stress severity and correlates with yield maintenance under water deficit.

The environmental adaptability of the YQSI is reflected in its robust performance across the contrasting climatic conditions of 2024 and 2025. The advantage of YQSI-selected varieties in yield and harvest index was even more pronounced under the more severe stress in 2025 (Table 1). This suggests that the YQSI is not only suitable for general drought screening, but can also identify genuinely stress-tolerant germplasms under extreme climatic events, aligning with the view of Tardieu [30] that the value of any drought-related trait depends on the specific drought scenario, and that traits should be evaluated under the target environment, rather than under a single standardized condition. By coupling yield and filling efficiency, YQSI is precisely adapted to drought scenarios characterized by combined stress during grain filling, which traditional yield-oriented indices find difficult to achieve.

From a breeding perspective, the physiological interpretation of the YQSI has practical implications. The index does not require physiological measurements such as enzyme activities or carbon isotope discrimination, which are costly and time-consuming to obtain. Instead, it uses BGR, a trait that can be derived from standard agronomic measurements, as a proxy for filling efficiency. This makes the YQSI readily applicable in breeding programs without additional specialized equipment. The six strongly drought-resistant germplasms identified in this study (Gigu 19, Gigu 39, Zhangzagu 18, Zhangzagu 16, Yugu 35 and Jigu 19) exhibited consistently superior performance in both yield and BGR across years, suggesting that they possess stable genetic mechanisms for maintaining assimilate transport and starch synthesis under drought. These germplasms provide valuable genetic resources for further physiological and molecular dissection of drought-tolerance mechanisms in foxtail millet.

### *4.3. Prediction Feasibility of Predicting YQSI Using UAV-Based Multimodal Remote Sensing Data and Machine Learning*

This study validated the feasibility of predicting the YQSI after heading in foxtail millet using UAV multimodal data and the Random Forest (RF) algorithm. The model achieved good prediction accuracy on the test set ($R^2 = 0.8193$). More importantly, the performance in screening drought-resistant varieties based on predicted YQSI was excellent, with an F1 score of 0.933 in both years.

Compared with previous studies, the advantage of this study lies in directly predicting a comprehensive index that integrates yield and quality (blighted grain rate), rather than merely predicting yield or evaluating drought-resistance grades. For example, Li et al. [11] used a multimodal data fusion model to predict a wheat drought-resistance index and achieved high accuracy, but their index was still centred on yield. Zhu et al. [25] used UAV multi-source data to construct a comprehensive evaluation index (D-value) for wheat drought resistance, which could effectively distinguish different drought-resistance grades, but the evaluation of this comprehensive index still required validation using traditional traits such as final yield. This study directly targets YQSI for prediction; the index already embeds yield and quality information, making the prediction results more directly valuable for breeding selection.

A fundamental question that needs to be addressed is why UAV remote sensing data can predict a composite index that simultaneously contains yield and quality information. We argue that this involves the coupling between canopy optical properties and grain-filling physiology. At the physical level, multispectral vegetation indices such as NDVI and WDRVI are closely related to leaf-area index and chlorophyll content, which directly determine canopy photosynthetic capacity and thus influence yield potential. This is consistent with the well-established relationship between NDVI and biomass accumulation [31,32]. At the physiological level, thermal infrared canopy temperature (NRCT) is a sensitive indicator of plant water status [33]. Water deficit during grain filling simultaneously reduces photosynthetic rate and assimilate-transport efficiency, leading to canopy warming and incomplete grain filling. These two pathways occur synchronously in time and are co-localized in the canopy in space. UAV multimodal data can, therefore, indirectly capture signals of grain-filling quality. In addition, texture features such as RE_MEA reflect the spatial heterogeneity of canopy structure, capturing patchy senescence induced by drought stress. This is a canopy-level manifestation of uneven grain filling, which is directly related to the BGR component of YQSI. This mechanistic explanation is consistent with the findings of Wu et al. [27] and Li et al. [11] in UAV-based prediction of yield and drought-resistance indicators, but the unique contribution of this study is the demonstration that remote sensing signals can simultaneously capture information from both yield and quality dimensions.

The feature-importance ranking revealed the key remote sensing variables controlling YQSI prediction. NDVI ranked first with 5.88% importance, consistent with its role as a core indicator of canopy greenness and photosynthetic capacity. WDRVI (5.43%) and RE_MEA (5.38%) followed closely. WDRVI is more sensitive to vegetation signals over a wide dynamic range [34], while RE_MEA reflects texture information in the red-edge band. The red edge is the transition zone between chlorophyll absorption and near-infrared reflectance, and its texture features are highly sensitive to changes in canopy structure and leaf angle. Notably, the top five features (NDVI, WDRVI, RE_MEA, NRCT, and RVI) cumulatively contributed approximately 26.5% of the total importance, with a relatively even distribution. No single feature dominated. This pattern indicates that YQSI prediction relies on the complementarity of multi-dimensional information, with spectral, textural, and thermal features all contributing. This, in turn, validates the necessity of a multimodal data fusion strategy. It should be noted that the purpose of using the RF algorithm in this study is not to identify the optimal prediction model, but to validate the fundamental assumption that machine learning can achieve YQSI prediction. RF's built-in feature selection and resistance to overfitting make it suitable as a proof-of-concept tool, while multi-model comparison and hyperparameter optimization are directions for future improvement.

The prediction accuracy under the non-watered treatment ($R^2 = 0.614$) was lower than under deficit-irrigated and well-watered treatments. This pattern is common in similar studies. Extreme drought-induced canopy senescence and leaf rolling cause spectral–physiological relationships to deviate from normal trajectories (11; 25). Error analysis indicated that approximately 11% of samples contributed the majority of prediction errors, with these samples mostly coming from genotypes with abnormal canopy architecture. Nevertheless, the F1 score for variety screening based on predicted YQSI reached 0.933, indicating that the current error level has limited substantive impact on variety screening decisions. However, it should be clearly stated that the data split in this study used stratified random sampling based on yield level, and all F1 scores were calculated on an independent test set, avoiding resubstitution bias. Nevertheless, different replicates of the same variety may be distributed across training and test sets, which could lead to overestimation of model generalization ability. Therefore, before extending this model to independent years, locations, and germplasm populations, its predictive reliability should be regarded as requiring validation, rather than having been established.

### 4.4. Limitations and Future Perspectives

Several limitations of this study need to be explicitly acknowledged. First, the YQSI currently incorporates only BGR as a quality constraint, whereas foxtail millet quality also includes dimensions such as protein content, starch composition, and taste quality [35]. This means that varieties selected by the YQSI have advantages in grain-filling completeness, but their performance on other quality dimensions has not been verified. The practical implication of this limitation is that YQSI is currently better suited as an early-generation screening tool in breeding programs, rather than as a substitute for refined quality evaluation.

Second, prediction accuracy under extreme drought conditions still has room for improvement, and the current validation is limited to a single location and two years of data. This means that the cross-environment generalizability of the model has not been established. The reliability of this model in practical breeding programs requires independent validation across multiple locations and years.

Third, the construction and validation of the YQSI are based on foxtail millet as a specific crop. Its applicability to other crops such as wheat, maize, and sorghum remains to be tested. The grain-filling physiology and drought-resistance strategies differ among crops, and the effectiveness of BGR as a quality constraint may vary across species. However, the design logic of the YQSI, deducting filling defects from yield advantage, is transferable across crops, because grain-filling completeness is a common quality dimension for all cereal crops.

Looking forward, three directions merit priority attention. First, incorporating additional quality dimensions into the YQSI framework, such as protein content estimated via near-infrared spectroscopy, to construct a comprehensive evaluation system with multi-dimensional quality constraints. Second, validating the screening efficacy of YQSI and the predictive generalization of the model in independent years, multiple locations, and larger germplasm populations. This is a necessary prerequisite for translating the YQSI from a research tool into a breeding screening tool. Third, systematically comparing multiple machine-learning algorithms, including deep-learning models, for YQSI prediction, and introducing time-series remote sensing data to capture grain-filling dynamics. This approach is expected to further improve prediction accuracy under extreme conditions.

Ultimately, this study demonstrates that incorporating quality dimensions into drought-resistance evaluation is not only methodologically feasible, but also of substantial practical value in breeding. It provides breeders with quality-differentiating information beyond yield without increasing screening costs. This is of significant importance for improving variety development efficiency in arid and semi-arid regions.

## 5. Conclusions

This study constructed the Yield–Quality Synergy Index (YQSI) to address the neglect of grain quality in conventional foxtail millet drought-resistance evaluation. The index penalizes varieties with poor grain filling while retaining yield potential, and its simple subtraction formula is robust to weight selection, with variety rankings remaining stable across a four-fold range of quality-penalty weights. Compared with eight traditional indices across two years, the YQSI tied with DYI for first place in comprehensive screening performance, while achieving the highest inter-annual stability (Spearman $\rho = 0.823$, composite score = 1.261), and introduced meaningful internal re-ranking among yield-similar varieties based on independently measured grain-filling quality. Six germplasms (Gigu 19, Gigu 39, Zhangzagu 18, Zhangzagu 16, Yugu 35 and Jigu 19) were identified as strongly drought-resistant; among them, Zhangzagu 16 and Gigu 19 consistently showed high yield with moderate BGR, while Yugu 35 and Jigu 19 demonstrated stable performance across water regimes and years, making them suitable as parents for breeding programs targeting both yield stability and grain-filling quality.

Using UAV multimodal data and Random Forest, the YQSI was predicted with an overall $R^2$ of 0.819 on the test set, and screening based on predicted YQSI achieved an F1 score of 0.933 (calculated on the independent test set), confirming the feasibility of UAV-based high-throughput phenotyping for this index. Feature-importance analysis identified NDVI, WDRVI, and red-edge texture (RE_MEA) as the most influential predictors. However, the model has been validated only within a single-location two-year experiment; its generalization to independent years, environments, and germplasm populations requires further validation. Future work should proceed in three phases: short-term optimization of prediction through multi-algorithm comparison and time-series remote sensing data, medium-term extension to additional quality dimensions and multi-location validation, and long-term multi-omics dissection of the six identified germplasms to reveal molecular mechanisms underlying their stable drought resistance and superior filling efficiency. This study provides a quality-constrained drought-resistance evaluation framework for foxtail millet and demonstrates a practical pathway for accelerating variety improvement in arid and semi-arid regions.

**Author Contributions:** J.Q.: writing—original draft; writing—review and editing; visualization; validation; formal analysis; supervision. J.L.: resources; data curation; conceptualization; visualization; validation; methodology; investigation. Y.W. (Yongfeng Wu): writing—review and editing, methodology, conceptualization. W.Q.: validation, formal analysis. W.Z.: investigation, resources, project administration, funding acquisition, writing—review and editing. B.W.: validation, resources. Z.C.: resources, data curation. B.L.: formal analysis, data curation. Y.L.: validation, data curation. Y.W. (Youqi Wang): visualization. B.Y.: investigation, resources, project administration, writing—review and editing. All authors have read and agreed to the published version of the manuscript.

**Funding:** This research was funded by the China Agricultural Research System (CARS-06-14.5-A34), Hebei Agriculture Research System (HARS-HBCT2024080202), and Hebei Agriculture Research System, grant number 2026KJCXZX-HZS-7.

**Data Availability Statement:** The original contributions presented in this study are included in the article. Further inquiries can be directed to the corresponding author.

**Acknowledgments:** We are grateful to the editors and anonymous reviewers for their insightful comments and constructive suggestions, which have significantly improved the quality of this manuscript. We thank the School of Geographical Sciences, Hunan Normal University; the Institute of Environment and Sustainable Development in Agriculture, Chinese Academy of Agricultural Sciences; the Dryland Farming Institute, Hebei Academy of Agriculture and Forestry Sciences/Key Laboratory of Crop Drought Tolerance Research of Hebei Province; and the Dayu College, Hohai University, for providing experimental sites, research facilities, and personnel support. This work was financially supported by the China Agricultural Research System (CARS-06-14.5-A34), the Hebei Agriculture Research System (HARS-HBCT2024080202), and the Hebei Agriculture Research System (grant number 2026KJCXZX-HZS-7). The funders had no role in study design, data collection, analysis, or manuscript preparation.

**Conflicts of Interest:** The authors declare no conflicts of interest.

## Appendix A

**Table A1.** List of features for random forest model construction.

| Category | Feature | Description/Formula | Reference |
|---|---|---|---|
| Colour Index | ExG | Excess Green Index: $ExG = 2g - r - b$ | [36] |
| | ExGR | Excess Green minus Red Index: $ExGR=3g - 2.4r - b$ | [37] |
| | GRVI | Green-Red Vegetation Index: $GRVI=\frac{g - r}{g + r}$ | [38] |
| Spectral Index | DVI | Difference Vegetation Index: $DVI=NIR - R$ | [31] |
| | EVI2 | Two-band Enhanced-Vegetation Index: $EVI2=2.5\times\frac{NIR - R}{NIR+2.4\times R+1}$ | [39] |
| | GCI | Green Chlorophyll Index: $GCI=\frac{NIR}{G} - 1$ | [40] |
| | GNDVI | Green Normalized-Difference Vegetation Index: $GNDVI=\frac{NIR - G}{NIR+G}$ | [41] |
| | IPVI | Infrared Percentage Vegetation Index: $IPVI=\frac{NIR}{NIR+R}$ | [42] |
| | MCARI | Modified Chlorophyll Absorption in Reflectance Index: $MCARI=[(RE - R) - 0.2\times(RE - G)]\times\{R\}$ | [43] |
| | MCARI/OSAVI | Ratio of MCARI to OSAVI: $MCARI/OSAVI=\frac{MCARI}{OSAVI}$ | [43] |
| | MSAVI | Modified Soil-Adjusted Vegetation Index: $MSAVI=\frac{2\times NIR+1-\sqrt{(2\times NIR+1)^2 - 8\times(NIR - R)}}{2}$ | [44] |
| | MSR | Modified Simple Ratio: $MSR=\frac{\sqrt{\frac{NIR}{R}} - 1}{\sqrt{\frac{NIR}{R}}+1}$ | [45] |

https://doi.org/10.3390/agriculture16161765

| | | | |
|---|---|---|---|
| | NDRE | Normalized-Difference Red Edge: $NDRE=\frac{NIR-RE}{NIR+RE}$ | [46] |
| | NDREI | Normalized-Difference Red-Edge Index (using RE and G): $NDREI=\frac{RE-G}{RE+G}$ | [47] |
| | NDVI | Normalized-Difference Vegetation Index: $NDVI=\frac{NIR-R}{NIR+R}$ | [32] |
| | OSAVI | Optimized Soil-Adjusted Vegetation Index: $OSAVI=\frac{NIR-R}{NIR+R+0.16}$ | [48] |
| | RECI | Red-Edge Chlorophyll Index: $RECI=\frac{NIR}{RE}-1$ | [40] |
| | RVI | Ratio Vegetation Index: $RVI=\frac{NIR}{R}$ | [31] |
| | SAVI | Soil-Adjusted Vegetation Index: $SAVI=1.5\times\frac{NIR-R}{NIR+R+0.5}$ | [49] |
| | WDRVI | Wide Dynamic-Range Vegetation Index: $WDRVI=\frac{0.12\times NIR-R}{0.12\times NIR+R}$ | [34] |
| Texture Feature (Red Band) | R_MEA | Mean (GLCM): $MEA=\sum_{i=0}^{N-1}\sum_{j=0}^{N-1} i\times P(i,j)$ | [50] |
| | R_VAR | Variance (GLCM): $VAR=\sum_{i=0}^{N-1}\sum_{j=0}^{N-1}(i-\mu)^2\times P(i,j)$ | [50] |
| | R_HOM | Homogeneity (GLCM): $HOM=\sum_{i=0}^{N-1}\sum_{j=0}^{N-1}\times\frac{P(i,j)}{1+\lvert i-j\rvert}$ | [50] |
| | R_CON | Contrast (GLCM): $CON=\sum_{i=0}^{N-1}\sum_{j=0}^{N-1}\lvert i-j\rvert^2\times P(i,j)$ | [50] |
| | R_DIS | Dissimilarity (GLCM): $DIS=\sum_{i=0}^{N-1}\sum_{j=0}^{N-1}\lvert i-j\rvert\times P(i,j)$ | [51] |
| | R_ENT | Entropy (GLCM): | [50] |

| | | | |
|---|---|---|---|
| | | $ENT=-\sum_{i=0}^{N-1}\sum_{j=0}^{N-1}P(i,j)\times\log P(i,j)$ | |
| | R_SEM | Second Moment (GLCM): $SEM=\sum_{i=0}^{N-1}\sum_{j=0}^{N-1}i^2\times P(i,j)$ | [50] |
| | R_COR | Correlation (GLCM): $COR=\sum_{i=0}^{N-1}\sum_{j=0}^{N-1}\frac{(i-\mu_i)(j-\mu_j)\times P(i,j)}{\sigma_i\sigma_j}$ | [50] |
| Texture Feature (Green Band) | G_MEA | Mean (GLCM)—formula same as R_MEA | [50] |
| | G_VAR | Variance (GLCM)—formula same as R_VAR | [50] |
| | G_HOM | Homogeneity (GLCM)—formula same as R_HOM | [50] |
| | G_CON | Contrast (GLCM)—formula same as R_CON | [50] |
| | G_DIS | Dissimilarity (GLCM)—formula same as R_DIS | [51] |
| | G_ENT | Entropy (GLCM)—formula same as R_ENT | [50] |
| | G_SEM | Second Moment (GLCM)—formula same as R_SEM | [50] |
| | G_COR | Correlation (GLCM)—formula same as R_COR | [50] |
| Texture Feature (Red-Edge Band) | RE_MEA | Mean (GLCM)—formula same as R_MEA | [50] |
| | RE_VAR | Variance (GLCM)—formula same as R_VAR | [50] |
| | RE_HOM | Homogeneity (GLCM)—formula same as R_HOM | [50] |
| | RE_CON | Contrast (GLCM)—formula same as R_CON | [50] |
| | RE_DIS | Dissimilarity (GLCM)—formula same as R_DIS | [51] |
| | RE_ENT | Entropy (GLCM)—formula same as R_ENT | [50] |
| | RE_SEM | Second Moment (GLCM)—formula same as R_SEM | [50] |
| | RE_COR | Correlation (GLCM)—formula same as R_COR | [50] |

| | | | |
|---|---|---|---|
| Texture Feature (NIR Band) | NIR_MEA | Mean (GLCM)—formula same as R_MEA | [50] |
| | NIR_VAR | Variance (GLCM)—formula same as R_VAR | [50] |
| | NIR_HOM | Homogeneity (GLCM)—formula same as R_HOM | [50] |
| | NIR_CON | Contrast (GLCM)—formula same as R_CON | [50] |
| | NIR_DIS | Dissimilarity (GLCM)—formula same as R_DIS | [51] |
| | NIR_ENT | Entropy (GLCM)—formula same as R_ENT | [50] |
| | NIR_SEM | Second Moment (GLCM)—formula same as R_SEM | [50] |
| | NIR_COR | Correlation (GLCM)—formula same as R_COR | [50] |
| Temperature Index | NRCT | Normalized Relative Canopy Temperature: $NRCT=\frac{T_c - T_{cmin}}{T_{cmax} - T_{cmin}}$ | [33] |

## References


1. Amadou, I.; Gounga, M.E.; Shi, Y.H.; Le, G.W. Fermentation and heat-moisture treatment induced changes on the physicochemical properties of foxtail millet (*Setaria italica*) flour. *Food Bioprod. Process.* **2014**, *92*, 38–45.
2. Zhang, W.; Wang, B.; Liu, B.; Chen, Z.; Lu, G.; Ge, Y.; Bai, C. Trait selection for yield improvement in foxtail millet (*Setaria italica* Beauv.) under climate change in the North China Plain. *Agronomy* **2022**, *12*, 1500.
3. Daryanto, S.; Wang, L.; Jacinthe, P.A. Global synthesis of drought effects on maize and wheat production. *PLoS ONE* **2016**, *11*, e0156362.
4. Farooq, M.; Hussain, M.; Siddique, K.H.M. Drought stress in wheat during flowering and grain-filling periods. *Crit. Rev. Plant Sci.* **2014**, *33*, 331–349.
5. Bouslama, M.; Schapaugh, W.T. Stress tolerance in soybean. Part 1: Evaluation of three screening techniques for heat and drought tolerance. *Crop Sci.* **1984**, *24*, 933–937.
6. Fischer, R.A.; Maurer, R. Drought resistance in spring wheat cultivars. I. Grain yield responses. *Aust. J. Agric. Res.* **1978**, *29*, 897–912.
7. Raman, A.; Verulkar, S.; Mandal, N.; Varia, M.; Shukla, V.; Dwivedi, J.; Singh, B.; Singh, O.; Swain, P.; Mall, A.; et al. Drought yield index to select high yielding rice lines under different drought stress severities. *Rice* **2012**, *5*, 31.
8. Rosielle, A.A.; Hamblin, J. Theoretical aspects of selection for yield in stress and non-stress environment. *Crop Sci.* **1981**, *21*, 943–946.
9. Fernandez, G.C.J. Effective selection criteria for assessing plant stress tolerance. In *Proceedings of the International Symposium on Adaptation of Vegetables and Other Food Crops to Temperature and Water Stress*; Kuo, C.G., Ed.; AVRDC Publication: Tainan, Taiwan, 1992; pp. 257–270.
10. Bidinger, F.R.; Mahalakshmi, V.; Rao, G.D.P. Assessment of drought resistance in pearl millet (*Pennisetum americanum*). I. Factors affecting yields under stress. *Aust. J. Agric. Res.* **1987**, *38*, 37–48.
11. Li, G.; Zhou, B.; Ni, M.; Chen, H.; Liu, Y.; Zhang, Y.; Zhang, M.; Wang, M. Stages-based multimodal data fusion model (S-MDFM) for wheat yield prediction and screening of drought-resistant and high-yield varieties. *Comput. Electron. Agric.* **2025**, *239*, 111122.

12. Mohammadi, R. Efficiency of yield-based drought tolerance indices to identify tolerant genotypes in durum wheat. *Euphytica* **2016**, *211*, 71–89.
13. Sadeghi, M.H.; Zakaria, R.A.; Mohammadi, S.A.; Sofalian, O.; Aharizad, S. An integrated index-based and multivariate approach for evaluating drought resilience in the CIMCOG wheat. *Field Crops Res.* **2025**, *312*, 109615.
14. Jaishreepriyanka, R.; Ravikesavan, R.; Iyanar, K.; Uma, D.; Senthil, N. Exploring the usefulness of drought tolerance indices in screening of maize inter-racial derivatives. *Electron. J. Plant Breed.* **2025**, *16*, 112–124.
15. Polania, J.; Rao, I.M.; Cajiao, C.; Rivera, M.; Raatz, B.; Beebe, S. Evaluation of drought indices to identify tolerant genotypes in common bean bush (*Phaseolus vulgaris* L.). *J. Integr. Agric.* **2020**, *19*, 99–110.
16. Barnabás, B.; Jäger, K.; Fehér, A. The effect of drought and heat stress on reproductive processes in cereals. *Plant Cell Environ.* **2008**, *31*, 11–38.
17. Yang, J.; Zhang, J. Grain filling of cereals under soil drying. *New Phytol.* **2006**, *169*, 223–236.
18. Liu, T.; Ji, C.; Wu, W.; Chen, W.; Yang, B.; Chen, C.; Sun, C.; Zhu, X.; Guo, W. Measurement of rice filled grain percentage based on grain shadow features. *Agron. J.* **2016**, *108*, 1234–1243.
19. Liu, T.; Wu, W.; Chen, W.; Sun, C.; Chen, C.; Wang, R.; Zhu, X.; Guo, W. A shadow-based method to calculate the percentage of filled rice grains. *Biosyst. Eng.* **2016**, *150*, 79–88.
20. Li, L.; Mao, Z.; Wang, P.; Cai, J.; Zhou, Q.; Zhong, Y.; Jiang, D.; Wang, X. Drought priming enhances wheat grain starch and protein quality under drought stress during grain filling. *J. Integr. Agric.* **2025**, *24*, 2888–2901.
21. Vadez, V.; Grondin, A.; Chenu, K.; Henry, A.; Laplaze, L.; Millet, E.J.; Carminati, A. Crop traits and production under drought. *Nat. Rev. Earth Environ.* **2024**, *5*, 311–326.
22. Zhao, X.; Huang, M.; Huang, X.; Liu, E. Evaluation of drought resistance and index screening of foxtail millet cultivars. *J. Water Clim. Change* **2023**, *14*, 2384–2396.
23. Liu, J.; Wu, Y.; Ma, J.; Liu, B.; Zhang, W.; Zhao, Y. Estimation of leaf, spike, stem and total biomass of winter wheat under water-deficit conditions using UAV multimodal data and machine learning. *Remote Sens.* **2025**, *17*, 2562.
24. Qin, J.; Zhang, Y.; Wu, Y.; Fu, W.; Song, Z.; Zhang, G.; Zhang, Y.; Liu, J.; Yang, B. Early-stage recognition of common ragweed (*Ambrosia artemisiifolia* L.) using low-cost UAV RGB imagery and deep learning. *Smart Agric. Technol.* **2026**, *14*, 102032.
25. Zhu, X.; Liu, X.; Wu, Q.; Liu, M.; Hu, X.; Deng, H.; Zhang, Y.; Qu, Y.; Wang, B.; Gou, X.; et al. Utilizing UAV-based high-throughput phenotyping and machine learning to evaluate drought resistance in wheat germplasm. *Comput. Electron. Agric.* **2025**, *237*, 110602.
26. Kyratzis, A.C.; Skarlatos, D.P.; Menexes, G.C.; Vamvakousis, V.F.; Katsiotis, A. Assessment of vegetation indices derived by UAV imagery for durum wheat phenotyping under a water limited and heat stressed Mediterranean environment. *Front. Plant Sci.* **2017**, *8*, 1114.
27. Wu, Y.; Ma, J.; Zhang, W.; Sun, L.; Liu, Y.; Liu, B.; Wang, B.; Chen, Z. Rapid evaluation of drought tolerance of winter wheat cultivars using multi-criteria comprehensive evaluation based on UAV multispectral and thermal images and automatic noise removal. *Comput. Electron. Agric.* **2024**, *218*, 108679.
28. Hay, R.K.M. Harvest index: A review of its use in plant breeding and crop physiology. *Ann. Appl. Biol.* **1995**, *126*, 197–216.
29. Breiman, L. Random forests. *Mach. Learn.* **2001**, *45*, 5–32.
30. Tardieu, F. Any trait or trait-related allele can confer drought tolerance: Just design the right drought scenario. *J. Exp. Bot.* **2012**, *63*, 25–31.
31. Tucker, C.J. Red and photographic infrared linear combinations for monitoring vegetation. *Remote Sens. Environ.* **1979**, *8*, 127–150.
32. Rouse, J.W.; Haas, R.H.; Schell, J.A.; Deering, D.W. Monitoring vegetation systems in the Great Plains with ERTS. In Proceedings of the NASA Goddard Space Flight Center 3d ERTS-1 Symposium, Washington, DC, USA, 10–14 December 1974; Volume 1, pp. 309–317.
33. Li, J.; Schachtman, D.P.; Creech, C.F.; Wang, L.; Ge, Y.; Shi, Y. Evaluation of UAV-derived multimodal remote sensing data for biomass prediction and drought tolerance assessment in bioenergy sorghum. *Crop J.* **2022**, *10*, 1363–1375.
34. Gitelson, A.A. Wide dynamic range vegetation index for remote quantification of biophysical characteristics of vegetation. *J. Plant Physiol.* **2004**, *161*, 165–173.
35. Ma, K.; Yuan, X.Y.; Jia, Z.; Lu, H.Y.; Chen, X.Y.; Wen, X.Y.; Chen, F. Changes in the grain quality of foxtail millet released in China from the 1970s to the 2020s. *Food Res. Int.* **2025**, *209*, 116316.
36. Han, X.; Wang, H.; Yuan, T.; Zou, K.; Liao, Q.; Deng, K.; Zhang, Z.; Zhang, C.; Li, W. A rapid segmentation method for weed based on CDM and ExG index. *Crop Prot.* **2023**, *165*, 106189.

37. Chen, P.; Wang, F. Effect of crop spectra purification on plant nitrogen concentration estimations performed using high-spatial-resolution images obtained with unmanned aerial vehicles. *Field Crops Res.* **2022**, *288*, 108708.
38. Zhu, L.H.; Liu, X.N.; Wang, Z.; Tian, L.W. High-precision sugarcane yield prediction by integrating 10-m Sentinel-1 VOD and Sentinel-2 GRVI indexes. *Eur. J. Agron.* **2023**, *150*, 126889.
39. Jiang, Z.; Huete, A.R.; Didan, K.; Miura, T. Development of a two-band enhanced vegetation index without a blue band. *Remote Sens. Environ.* **2008**, *112*, 3833–3845.
40. Gitelson, A.A. Remote estimation of canopy chlorophyll content in crops. *Geophys. Res. Lett.* **2005**, *32*, L08403.
41. Gitelson, A.A.; Viña, A.; Arkebauer, T.J.; Rundquist, D.C.; Keydan, G.; Leavitt, B. Relationships between leaf chlorophyll content and spectral reflectance and algorithms for non-destructive chlorophyll assessment in higher plant leaves. *J. Plant Physiol.* **2003**, *160*, 271–282.
42. Crippen, R.E. Calculating the vegetation index faster. *Remote Sens. Environ.* **1990**, *34*, 71–73.
43. Daughtry, C.S.T.; Walthall, C.L.; Kim, M.S.; de Colstoun, E.B.; McMurtrey, J.E. Estimating corn leaf chlorophyll concentration from leaf and canopy reflectance. *Remote Sens. Environ.* **2000**, *74*, 229–239.
44. Qi, J.; Chehbouni, A.; Huete, A.R.; Kerr, Y.H.; Sorooshian, S. A modified soil adjusted vegetation index. *Remote Sens. Environ.* **1994**, *48*, 119–126.
45. Haboudane, D.; Miller, J.R.; Pattey, E.; Zarco-Tejada, P.J.; Strachan, I.B. Hyperspectral vegetation indices and novel algorithms for predicting green LAI of crop canopies: Modeling and validation in the context of precision agriculture. *Remote Sens. Environ.* **2004**, *90*, 337–352.
46. Gitelson, A.A.; Merzlyak, M.N. Remote estimation of chlorophyll content in higher plant leaves. *Int. J. Remote Sens.* **1997**, *18*, 2691–2697.
47. Muhammad, H.; Yang, M.; Rasheed, A.; Jin, X.; Xia, X.; Xiao, Y.; He, Z. Time-Series Multispectral Indices from Unmanned Aerial Vehicle Imagery Reveal Senescence Rate in Bread Wheat. *Remote Sens.* **2018**, *10*, 809.
48. Rondeaux, G.; Steven, M.; Baret, F. Optimization of soil-adjusted vegetation indices. *Remote Sens. Environ.* **1996**, *55*, 95–107.
49. Huete, A.R. A soil-adjusted vegetation index (SAVI). *Remote Sens. Environ.* **1988**, *25*, 295–309.
50. Haralick, R.M.; Shanmugam, K.; Dinstein, I. Textural features for image classification. *IEEE Trans. Syst. Man Cybern.* **1973**, *SMC-3*, 610–621.
51. Clausi, D.A. An analysis of co-occurrence texture statistics as a function of grey level quantization. *Can. J. Remote Sens.* **2002**, *28*, 45–62.